Strategies and Mechanisms of Cellular Interaction between the Parasitic Weed *Orobanche cumana* WALLR. and its Host *Helianthus annuus* L.

Dissertation for Obtaining the Doctoral Degree
of Natural Sciences (Dr. rer. nat.)

Faculty of Natural Sciences
University of Hohenheim

Institute of Botany
Biodiversity and Plant Interaction

submitted by
Anna Clarissa Krupp

from Aichwald
2020

Dean:	Prof. Dr. Uwe Beifuß
1st reviewer:	Prof. Dr. Otmar Spring
2nd reviewer:	Prof. Dr. Philipp Schlüter
Submitted on:	12.02.2020
Oral examination on:	13.05.2020

This work was accepted by the Faculty of Natural Sciences at the University of Hohenheim on 27.02.2020 as “Dissertation for Obtaining the Doctoral Degree of Natural Sciences”.

Time, "forgetting," and incubation are equally necessary before deep scientific or mathematical insights can be achieved.

Oliver Sacks (2017)

"The River of Consciousness"
Pan Macmillan, London

Table of contents

List of figures

List of abbreviations

app – appressorium / appressoria

ddH_2O – double distilled water

dpi – days post inoculation

germ – germination / germinated seeds

MeOH – methanol

n – number / sample size

p – *p*-value / probability value

SD – standard deviation

SE – sieve element

STL – sesquiterpene lactone/s

tub – tubercle/s

Species names

Parasites

Alectra vogelii (Orobanchaceae)

Cuscuta pentagona (Convolvulaceae) – fiveangled dodder, Seide / Teufelszwirn

Orobanche (Orobanchaceae)

O. cernua – nodding broomrape, Nickende Sommerwurz

O. crenata – bean broomrape, Gezähnelte Sommerwurz

O. cumana – sunflower broomrape, Sonnenblumen-Sommerwurz

Phelipanche (Orobanchaceae)

P. aegyptiaca – Egyptian broomrape, Ägyptische Sommerwurz

P. ramosa – branched / hemp broomrape, Ästige Sommerwurz

Striga (Orobanchaceae)

S. asiatica – Asiatic / red witchweed

S. hermonthica – purple witchweed

Hosts

Artemisia spp. (Asteraceae) – wormwoods, Beifuß-Arten

Helianthus annuus (Asteraceae) – sunflower, Sonnenblume

Vicia narbonensis (Fabaceae) – Narbon bean, Maus-Wicke

Summary

Sunflower broomrape, *Orobanche cumana* WALLR., is a root parasitic plant causing considerable yield losses in sunflower cultivation in Europe, North Africa and Asia. Comprehensive knowledge about the early interaction stages between host and parasite is necessary to find new ways of controlling this weed. In this thesis, three aspects regarding the biology of *O. cumana* were studied: 1) the chemotropism of *O. cumana* germtubes which bend towards the host root, 2) the development of *O. cumana* on resistant and susceptible sunflower lines and 3) the development of the phloem connection between the *O. cumana* haustorium and the sunflower host root.

Sesquiterpene lactones in sunflower root exudates act as germination stimulants for *O. cumana*. As sesquiterpene lactones are known inhibitors of plant elongation growth and seem to play a role in the phototropic curvature of sunflower hypocotyls, it was tested if they also serve as chemotropic signals for the host-finding of *O. cumana* germtubes. A chemotropism bioassay was established by placing filter discs with the substances of interest on water agar in petri dishes and recording the growth direction of emerging germtubes. When sesquiterpene lactone containing sunflower root exudate, sunflower seed oil extract or the sesquiterpene lactone reference costunolide were applied, 70 % of the germtubes showed orientation towards the filter discs. The artificial strigolactone GR24, however, did not induce chemotropism. A concentration gradient of sesquiterpene lactones exudated from the host root is likely to be responsible for a stronger inhibition of elongation growth on the host-facing flank of the germtube compared to the far side flank. This would confer a double role of sesquiterpene lactones from root exudates in the sunflower-broomrape-interaction, namely as germination stimulants and as chemotropic signals.

One way of controlling *O. cumana* is the cultivation of resistant sunflower lines. However, this resistance is rapidly overcome by more aggressive pathotypes of the parasite. Therefore, the resistance or tolerance reaction of the sunflower genotype T35001 was investigated in comparison to six other sunflower genotypes with different resistance characteristics. The development of *O. cumana* was monitored in a root chamber system which allowed permanent assessment of germination, attachment and tubercle formation in the different host-parasite-combinations. All seven tested sunflower lines induced germination and attachment of *O. cumana*, independent of the expected resistance or

susceptibility of the host. A difference between compatibility or incompatibility of the interactions was only observed at the tubercle stage. On T35001, tubercles never occurred, neither in root chamber experiments, nor in additional pot experiments. To find out why the development stopped before the tubercle stage, samples of sunflower roots with attached *O. cumana* seedlings were analysed by bright field- and fluorescence microscopy as well as transmission electron microscopy. Histological studies revealed that *O. cumana* penetrated the host root, but never reached the host's vascular bundle. The root cortex cells surrounding the *Orobanche* haustorium showed no ultrastructural changes such as cell wall thickening. Fluorescence microscopy revealed no callose depositions or signs of phytoalexin release. However, ultrastructural examination of the host-parasite-interface showed degeneration processes in both cortex and haustorial cells. Cortex cells were flooded with bacteria, haustorium cells showed degeneration of cytoplasm and nuclei. The resistance mechanism that prevented further development of the *O. cumana* haustorium did not express itself in a histologically visible way.

As holoparasite, *O. cumana* acquires its entire demand for water, minerals and organic nutrients from the host's vascular system. The development of the xylem connection between *O. cumana* and sunflower had previously been reported, but the phloem connection is far more relevant for the parasite in terms of organic nutrients. Accordingly, the ultrastructure of the phloem connection between the haustorium of young *O. cumana* tubercles and the sunflower root was examined. Parasite and host tissues were intermingled at the contact site and difficult to distinguish, but sieve-tube elements of *O. cumana* and sunflower could be differentiated according to their plastid ultrastructure. While sieve-element plastids of *O. cumana* were larger, often irregular in shape and contained few, small starch inclusions, sieve-element plastids of the host were significantly smaller, always round with more and larger starch inclusions. This made it possible to trace the exact contact site of host and parasite sieve elements to show a direct symplastic phloem connection between the two species. The interspecific sieve plate showed more callose on the host side. This allowed detection of newly formed plasmodesmata between host sieve-tube elements and parenchymatic parasite cells, thus showing that undifferentiated cells of the parasite can connect to fully differentiated sieve elements of sunflower.

Zusammenfassung

Die Sonnenblumen-Sommerwurz, *Orobanche cumana* WALLR., ist eine wurzelparasitische Pflanze, die beträchtliche Ernteausfälle im Sonnenblumenanbau in Europa, Nordafrika und Asien verursacht. Umfassendes Wissen über die frühen Interaktionsstadien zwischen Wirt und Parasit sind notwendig, um neue Wege zur Bekämpfung des Parasiten zu finden. In dieser Arbeit wurden drei Aspekte der Biologie von *O. cumana* untersucht: 1) Der Chemotropismus von *O. cumana*-Keimschläuchen hin zur Wirtswurzel; 2) die Entwicklung von *O. cumana* auf resistenten und suszeptiblen Sonnenblumen-Linien; und 3) die Entwicklung der Phloem-Verbindung zwischen dem *O. cumana*-Haustorium und der Sonnenblumen-Wirtswurzel.

Sesquiterpenlactone in Wurzelexsudaten der Sonnenblume induzieren die Keimung von *O. cumana*-Samen. Sie sind auch als Inhibitoren des pflanzlichen Streckungswachstums bekannt und scheinen eine Rolle in der phototropen Krümmung von Sonnenblumen-Hypokotylen zu spielen. Deshalb wurde getestet, ob sie auch als chemotrope Signale für die Wirtsfindung von *O. cumana*-Keimschläuchen verantwortlich sind. Ein Chemotropismus-Biotest wurde entwickelt, bei dem die Wuchsrichtung der Keimschläuche in Petrischalen mit Wasseragar und Testsubstanzen auf Filterplättchen erfasst wurde. Wenn sesquiterpenlactonhaltiges Sonnenblumenwurzelexsudat, Sonnenblumenölextrakt oder die Sesquiterpenlacton-Referenzsubstanz Costunolid eingesetzt wurden, wuchsen 70 % der Keimschläuche zu den Filterplättchen hin. Das künstliche Strigolacton GR24 induzierte keinen Chemotropismus. Ein Konzentrationsgradient der von der Wirtswurzel exsudierten Sesquiterpenlactone scheint für eine stärkere Inhibierung des Streckungswachstums auf der dem Wirt zugewandten Keimschlauchseite im Vergleich zur abgewandten Seite verantwortlich zu sein. Dies würde den Sesquiterpenlactonen in Sonnenblumenwurzelexsudaten eine Doppelrolle in der Interaktion mit *O. cumana* zukommen lassen, nämlich als Keimstimulanzien und als Signale für den Chemotropismus.

O. cumana kann durch den Anbau resistenter Sonnenblumenlinien bekämpft werden. Diese Resistenz wird jedoch von neuen, aggressiveren Pathotypen des Parasiten überwunden. Ziel war es daher, Resistenz- oder Toleranzreaktionen des Sonnenblumen-Genotyps T35001 im Vergleich zu sechs anderen Sonnenblumengenotypen mit unterschiedlichen Resistenzcharakteristika zu untersuchen. Ein Wurzelkammersystem erlaubte die kontinuierliche Beobachtung der Keimung, Anlagerung und Tuberkelbildung bei den unterschiedlichen Wirt-Parasit-Kombinationen. Alle sieben getesteten

Sonnenblumenlinien induzierten die Keimung und Anlagerung von *O. cumana*, unabhängig von deren erwarteter Suszeptibilität oder Resistenz. Ein Unterschied zwischen kompatiblen und inkompatiblen Interaktionen wurde erst im Tuberkelstadium sichtbar. Auf den Wurzeln von T35001 entwickelten sich nie Tuberkel, weder in Wurzelkammer- noch in Topfversuchen. Um herauszufinden, warum die Entwicklung von *O. cumana* vor dem Tuberkelstadium stoppte, wurden Proben von Sonnenblumenwurzeln mit angelagerten Keimlingen licht-, fluoreszenz- und transmissionselektronenmikroskopisch untersucht. Die histologischen Studien zeigten, dass der Parasit zwar in die Wirtswurzel eindrang, jedoch nicht den Zentralzylinder erreichte. Die Wurzelrindenzellen, die das *Orobanche*-Haustorium umgaben, wiesen keine ultrastrukturellen Veränderungen auf, wie beispielsweise Zellwandverdickungen. Weder Kalloseablagerungen noch Zeichen für Phytoalexinproduktion waren mittels Fluoreszenzmikroskopie sichtbar. Ultrastrukturelle Untersuchungen der Kontaktstellen von Wirt und Parasit zeigten jedoch Degenerationsprozesse sowohl in den Zellen der Wurzelrinde als auch in denen des Haustoriums. Die Wurzelzellen waren voller Bakterien und auch Zellkerne und Cytoplasma der Haustorienzellen erschienen degeneriert. Der Resistenzmechanismus, der die weitere Entwicklung des Haustoriums verhinderte, war histologisch nicht sichtbar.

Als Holoparasit deckt *O. cumana* seinen gesamten Bedarf an Wasser, Mineralien und organischen Nährstoffen aus dem Leitbündelsystem des Wirtes. In dieser Arbeit wurde zum ersten Mal die Ultrastruktur der Phloemverbindung zwischen dem Haustorium des jungen Tuberkels und der Wirtswurzel untersucht. Die Gewebe von Wirt und Parasit waren an den Kontaktstellen schwer zu unterscheiden. Jedoch konnten die Siebröhrenelemente aufgrund ihrer Plastidenultrastruktur eindeutig zugeordnet werden. Während die Siebröhrenplastiden von *O. cumana* meist größer und unregelmäßig geformt waren und wenige kleine Stärkeeinschlüsse enthielten, waren die Siebröhrenplastiden der Sonnenblume signifikant kleiner, immer rundlich und besaßen mehr und größere Stärkeeinschlüsse. Dies erlaubte es, die exakte Anschlussstelle zwischen Wirt und Parasit zu finden. Es wurden direkte symplastische Phloemverbindungen zwischen den beiden Arten entdeckt. Die interspezifische Siebplatte wies auf der Wirtsseite stets mehr Kallose auf und ermöglichte somit die Identifizierung neu gebildeter Plasmodesmen zwischen parenchymatischen Haustorienzellen und Siebröhren der Sonnenblume. Die undifferenzierten *Orobanche*-Zellen konnten sich also mit den vollständig differenzierten Siebröhrenelementen der Sonnenblume verbinden.

I. General introduction

Parasitic plants are fascinating organisms. Whereas normal plants produce their own nutrients via photosynthesis and take up water and minerals via roots, holoparasitic plants withdraw all needed substances from a host plant. This has led to a number of specific adaptations (Kuijt 1969, Heide-Jørgensen 2008, 2013). In comparison to non-parasites or hemiparasites, root holoparasites usually only have small scale-leaves, they lack chlorophyll and have no roots (Heide-Jørgensen 2008, 2013). Instead they connect to the roots of a host plant with a specialised organ, the haustorium, which functions as anatomical and physiological bridge between parasite and host (Kuijt 1969, Joel 2013, Yoshida *et al.* 2016). Via the haustorium, the parasite acquires its entire demand for water, minerals and organic nutrients from the host's vascular system (Westwood 2013). This causes a growth reduction of the host plant, which is particularly problematic in crop plants. Especially the root parasites of the Orobanchaeceae family pose a great threat to agriculture (Heide-Jørgensen 2013, Parker 2013). The genus *Striga* (witchweeds) causes considerable yield losses in Poaceae crops (e.g. maize, millet, rice) in sub-Saharan Africa. The genera *Orobanche* and *Phelipanche* (broomrapes) comprise many weedy species that attack a variety of crops, from families like the Solanaceae, Fabaceae, Apiaceae and Asteraceae (Koch 1887, Parker 2013). Most of these have a more or less wide host range and there is only one species with a single principal host crop: sunflower broomrape, *Orobanche cumana* WALLR. (Parker 2013).

O. cumana is a specific parasite of cultivated sunflower (*Helianthus annuus* L.). It is a serious and increasing threat to sunflower cultivation in the Old World, namely the Mediterranean, Eastern Europe and Asia, where it causes severe yield losses (Fig. I; Parker 2009, 2013, Fernández-Martínez *et al.* 2015). Interestingly, *O. cumana* is not present on the American continent (Cantamutto *et al.* 2014, Kaya 2014), where sunflower was domesticated by Native Americans (for references see Jan & Seiler 2007). *O. cumana* evolved in Russia, where sunflower was cultivated in the 18th century (Teryokhin 1997, Škorić *et al.* 2010, Antonova 2014, Moninero-Ruiz *et al.* 2015). First reports of sunflowers parasitised by *O. cumana* stem from the late 19th century (for references see Teryokhin 1997, Škorić *et al.* 2010, Antonova 2014). *O. cumana* putatively evolved from an *Orobanche cernua* LOEFL. population parasitising wild Asteraceae species, e.g. *Artemisia* spp. (Škorić *et al.* 2010, Antonova 2014, Fernández-Martínez *et al.* 2015). Now

O. cumana is mainly found on cultivated sunflower and differs genetically and morphologically from *O. cernua* (Kreutz 1995, Katzir *et al.* 1996, Pujadas-Salvà & Velasco 2000, Román *et al.* 2003).

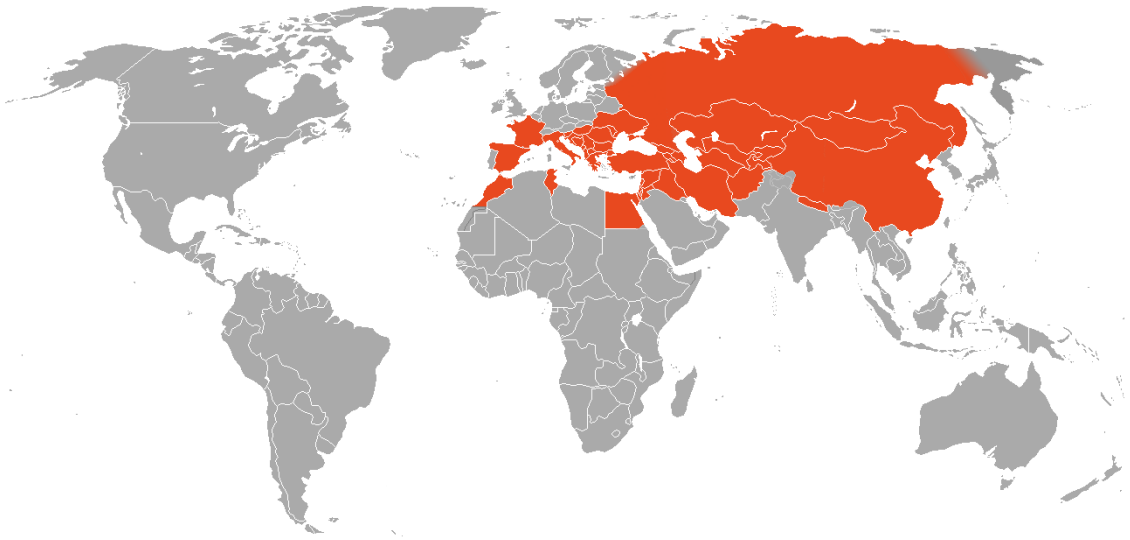

Fig. I Global distribution of *O. cumana*. Countries in which *O. cumana* has been reported are marked in red. Data based on Parker 2013 and Kreutz 1995, Amri *et al.* 2012, Antonova 2014, Jestin *et al.* 2014, Shi *et al.* 2015, Jebri *et al.* 2017, Nabloussi *et al.* 2017. Source of the blank map: https://upload.wikimedia.org/wikipedia/commons/4/46/BlankMap-World-2007.png.

The annual lifecycle of *O. cumana* is closely linked to the lifecycle of its host (Fig. II). The tiny seeds of the parasite germinate only when a suitable host root is nearby. Germination of the seeds is triggered by sesquiterpene lactones that are exudated into the soil by sunflower roots (Joel *et al.* 2011, Raupp & Spring 2013). The seedling of *O. cumana* is a hyaline tube that develops from hypocotyl and radicle tissues (Joel & Bar 2013). It lacks typical seedling structures and is therefore often called ‘germtube’ (Losner-Goshen *et al.* 1991, Joel & Losner-Goshen 1994, Delavault 2015). The germtube grows towards the host root (Krupp 2014, Fernández-Martínez *et al.* 2015). This directed growth has been studied in other species, where chemotropism was identified as the underlying mechanism (Saunders 1933, Whitney & Carsten 1981). When the germtube touches the host root, an attachment organ is formed, the appressorium (Krenner 1958, Joel & Losner-Goshen 1994). In a next step, the parasite penetrates the host root tissues and connects to the host’s vascular bundle, thus forming the haustorium (Dörr *et al.* 1994). Via this anatomical and physiological bridge, the parasite withdraws all needed substances from

its host (Teryokhin 1997, Westwood 2013, Delavault 2015, Fernández-Martínez *et al.* 2015). Organic nutrients are stored in a tubercle, from which the shoot arises (Koch 1887, Teryokhin 1997). The shoot emerges from the soil and starts flowering at about two weeks after emergence (Parker & Riches 1993). *O. cumana* seems to be mainly self-pollinated (Gagne *et al.* 1998), but cross-fertilization has also been observed (Rodríguez-Ojeda *et al.* 2013). Each flower develops into a capsule that contains hundreds of seeds, thus completing its lifecycle within approximately three to four months (Joel *et al.* 2007, Krupp 2014, Delavault 2015).

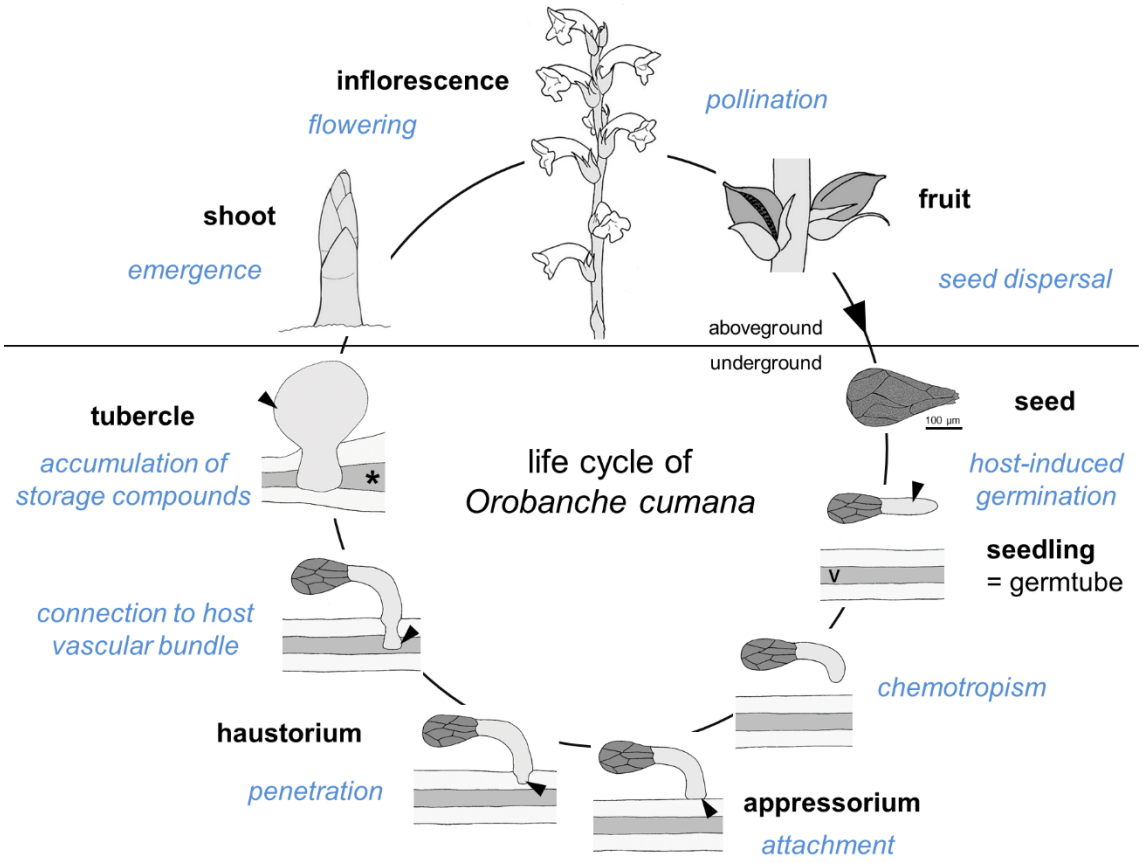

Fig. II Lifecycle of *O. cumana*. The parasite's organs are given in black and highlighted with arrowheads, processes are given in blue italics. The host root is depicted in a longitudinal section. *V* = vascular bundle of the host root, * = swelling of the host root upstream of the haustorium. Drawings by A. Krupp.

The seeds of *O. cumana* are approximately 300 µm long (Krupp *et al.* 2014) and are easily dispersed by wind, water, animals and agricultural machinery (Joel *et al.* 2007). The seeds remain viable in the soil for over a decade and with the massive amount of seeds produced by one plant a seedbank develops rapidly in the soil (Goldwasser & Rodenburg 2013). Heavy infestation of sunflower crop arises, with up to 86 parasites per host plant (Kreutz 1995), which can lead to a total yield loss (Joel *et al.* 2007). To control *O. cumana*, two main strategies have been implemented: cultivation of herbicide-resistant sunflower lines in an imidazol-system where all weeds including *O. cumana* are destroyed by herbicide application and breeding of sunflower lines that are resistant to *O. cumana* (Aly *et al.* 2001, Škorić *et al.* 2010, Fernández-Martínez *et al.* 2012). This resistance has however often been overcome by the parasite after a few years due to the occurrence of new, more aggressive physiological races or pathotypes (for definition of the terms see Spring *et al.* 2018) of *O. cumana* (Păcureanu-Joiţa *et al.* 2009, Škorić *et al.* 2010, Molinero-Ruiz *et al.* 2015).

Current research on the interaction of *O. cumana* and sunflower has mainly focused on the definition and distribution of new *O. cumana* pathotypes (Molinero-Ruiz *et al.* 2013, Pineda-Martos *et al.* 2013, Antonova 2014, Molinero-Ruiz *et al.* 2015, Duca *et al.* 2017), germination stimulants of the host (Joel *et al.* 2011, Raupp & Spring 2013, Ueno *et al.* 2014) and resistance genes of sunflower (Pérez-Vich *et al.* 2004, Velasco *et al.* 2007, Rodríguez-Ojeda *et al.* 2013, Imerovski *et al.* 2013, Molinero-Ruiz *et al.* 2015). In contrast, research on the fundamental processes of cellular interaction between host and parasite in the early developmental stages is relatively scarce.

However, the host-parasite-interaction has to be understood in detail to find new control strategies for this weed. The aim of this thesis was to investigate the strategies and mechanisms of the early interaction between *O. cumana* and its host sunflower. Thus, the following research questions arise:

1. How does the parasite’s germtube find the host root?

2. What mechanisms are responsible for sunflower resistance against *O. cumana*?

3. How does the parasite connect to the host’s phloem?

These research questions are addressed in the following three chapters to shed light on the biology of this economically relevant parasitic plant.

Chapter 1: Chemotropism of *O. cumana* germtubes

Some of the results presented in this chapter are part of the thesis for a teaching degree of Barbara Bertsch (2015) conducted under my co-supervision.

1. 1 Introduction

Chemical signals are decisive factors for the survival of parasitic plants. Thus, strigolactones and sesquiterpene lactones (STL) released from the hosts have been found to stimulate germination of root parasites from the Orobanchaceae family and secure host specificity (reviewed by Yoneyama *et al.* 2013). But germination is only the first step, which wakes up the parasite by breaking its dormancy. Afterwards, the parasite has to reach the host by actively growing towards it (Beck-Mannagetta 1890, Kadry & Tewfic 1956, Teryokhin 1997). The shoot parasite dodder (*Cuscuta pentagona* ENGELM.), for example, "smells" its host and its growth is guided by volatile compounds such as α-pinene (Runyon *et al.* 2006). This process, named chemotropism, is even harder to study when it happens below ground as in root parasites. Germination of these parasitic plants has extensively been studied, especially in the weedy species like *Striga* spp. (Cook *et al.* 1966, 1972, Siame *et al.* 1993), *Phelipanche ramosa* (L.) POMEL (Auger *et al.* 2012) and also the sunflower parasite *O. cumana* (Joel *et al.* 2011, Raupp & Spring 2013, Ueno *et al.* 2014). However, the mechanism that leads to the curvature of the parasites' germtube (a highly reduced seedling, see Joel & Bar 2013) towards the host root, is very poorly understood up to date. Early studies by Pearson (1913a, b) and Saunders (1933) reported a chemotropic mechanism leading to directed growth in *Striga* seedlings. This was confirmed by Williams (1961) and illustrated by Yoshida & Shirasu (2009). For other genera of the Orobanchaceae, chemotropism was observed in *Alectra vogelii* BENTH. (Botha 1948, Visser *et al.* 1977) and *Orobanche crenata* FORSSK. (Whitney & Carsten 1981, Aber & Sallé 1982). However, the chemical nature of the signalling compounds was not unravelled. There are several plant metabolites that have been identified as mediators in tropic responses. One group of compounds relevant for mediating auxin-induced growth in plants and inducing phototropic curvature of sunflower hypocotyls are STL (Spring & Hager 1981, Yokotani-Tomita *et al.* 1999, Ueda *et al.* 2013). Four of these STL, dehydrocostus lactone (Joel *et al.* 2011), costunolide, 8-epixanthatin and tomentosin, have recently been identified in root exudates of sunflower (*H. annuus*) as

germination stimulants for sunflower broomrape, *O. cumana* (Raupp & Spring 2013). Their potential role as chemotropic signal for the host finding process has not been investigated up to date. Therefore, the aim of this study was to establish a bioassay for testing the influence of target compounds on the growth of *O. cumana* germtubes and to test the hypothesis that the STL are the responsible chemotropic signal in the sunflower-broomrape-interaction.

1. 2 Material and methods

Plant material and cultivation

Sunflower (*Helianthus annuus* line HA300) plants were grown hydroponically in 1 l plastic containers for root exudate collection or co-cultivated with *O. cumana* seeds in a root chamber system (see chapter 3, p. 48 and Fig. 3.1, p. 49) to monitor germination and germtube orientation. Seeds of *O. cumana* pathotype G (collected in the Rostov region of Russia in 2012) were kindly provided by Dr. T. Antonova and PhD S. Guchetl (All-Russia Research Institute of Oil Crops by the name of V.S. Pustovoit, Laboratory of Immunity and Molecular Marking). In the germination bioassays, also *O. cumana* pathotype E+ (collected in Córdoba, Spain, in 2014) were used. *P. ramosa* seeds were collected in 2007 from tobacco fields in the Baden region in Germany.

Germination bioassay

Seeds of *O. cumana* and *P. ramosa* seeds were surface sterilised with 70 % ethanol for 1 min, 3.6 % sodium hypochlorite solution in 0.1 % Tween 80 for 3 min and 30 s in a supersonic bath, followed by 0.01 M hydrochloric acid for 10 min (method adapted from Conn *et al.* 2015). After each step, seeds were rinsed thoroughly with deionised water. The seeds were spread on a moist, heat sterilised Whatman filter (diameter 1.15 cm). For seed conditioning, these filter discs were kept on moist filter paper in Petri dishes at 18°C in darkness for at least one week. The conditioned seeds were put in small Petri dishes (diameter 3.8 cm) on Whatman filter discs containing 20 µl of germination stimulant. The filter paper at the bottom of each dish was moistened with 250 µl ddH_2O. Each Petri dish was sealed with Parafilm and wrapped in aluminium foil. After one week in the dark at 18°C, the seeds were germinated. The total seed number and number of germinated seeds were counted using photographs made with a digital camera (Canon PowerShot A640,

lens: Canon LA-DC 58F) mounted to a microscope (Zeiss Axioplan, Göttingen, Germany). The substances tested in germination bioassays were: sunflower seed oil; a methanolic extract of sunflower seed oil; the methanol extracted oil of sunflower; as well as olive oil, rape seed oil, mineral oil; the STL costunolide and dehydrocostus lactone; and the synthetic strigolactone GR24 (see below).

Chemotropism bioassay

The chemotropism bioassay (see Fig. 1.2) was performed in small petri dishes (diameter 3.8 cm) containing 1 % water agar (Agar Agar Kobe I, Roth, Karlsruhe, Germany). A heat sterilised 5 mm filter disc was immersed with 20 µl of the solved test substance, dried after application of the solvent and placed in the middle of the Petri dish. Under a dissecting microscope, conditioned *O. cumana* seeds (see above) were placed in a 90° angle to the filter with their micropyle alternatively pointing to the left and right in a concentric circle with 2 mm distance from the filter (Fig. 1.2 a, b). 10 µl of ddH_2O were pipetted onto the discs to allow dissolution and diffusion of the test substances. In tests with costunolide concentrations below 10^{-5} M, which were too low to induce germination in the distance, 10 µl of GR24 (1 ppm) dissolved in water was used instead of ddH_2O. The Petri dishes were sealed with parafilm and kept in the dark at 18°C. After 5–7 days, germtube curvature was recorded under a dissecting microscope. Germtubes bending towards the tested substance were recorded as positively chemotropic, germtubes bending away from it as negatively chemotropic, and germtubes with their tip not showing a clear direction as indeterminable (Fig. 1.2 c).

Additional tests were conducted: a) with a second concentric circle in 4 mm distance to the edge of the filter disc; b) with seeds evenly spread without distinctly positioned micropyles in a distance of 0–2 mm and 2–5 mm from the tested substance.

To test if the germtubes show gravitropism, an experiment was conducted with half of the Petri dishes placed bottom-up.

Samples tested in chemotropism bioassays were sunflower root exudate, methanolic extract of sunflower seed oil, costunolide and GR24.

Root exudate collection

Sunflower plants were grown hydroponically as described by Raupp & Spring (2013). Root exudates of 25 plants (four weeks old) were collected by pumping the water in which they were growing over a column filled with 5 g of the ion-exchange resin Amberlite (XD4, 20–60 mesh, matrix: styrene-divinylbenzene, 100 Å mean pore size, Sigma Aldrich, St. Louis, Missouri, USA) for 24 h at a flow rate of 0.35 ml/s. The exudate was washed out with acetone, dried, and resuspended in 1.5 ml acetone. The roots were dissected and weighed. The amount of exudate applied in germination and chemotropism bioassays corresponded to 0.1 g root fresh weight.

Sunflower oil extraction

Native, organic, cold pressed sunflower oil (Bio Planète, oil mill Moog, Lommatzsch, Germany) was extracted with methanol. 1 ml oil was mixed with 1 ml methanol in an Eppendorf tube, shaken, and kept for ca. 1 h until the two phases were separated again. The methanol phase was removed with a pipette and the extraction was repeated with 1 ml of methanol. 20 µl of the methanolic extract and of the remaining extracted oil were applied in the germination bioassay.

Other tested substances

The synthetic strigolactone GR24 ($C_{17}H_{14}O_5$) was purchased from B. Zwanenburg, Department of Organic Chemistry, Radboud University Nijmegen, Nijmegen, The Netherlands. GR24 was always used at a concentration of 1 ppm (= 3.3×10^{-6} M) in an aqueous solution. Costunolide ($C_{15}H_{20}O_2$) was purchased from Selleck Chemicals (Houston, TX, USA), dissolved and diluted in methanol. Dehydrocostus lactone ($C_{15}H_{18}O_2$) was purchased from Oskar Tropitzsch GmbH (Marktredwitz, Germany), dissolved in ethyl acetate and diluted with methanol.

Data collection and statistics

Germination percentages were calculated as germinated seeds per total number of seeds. At least three biological replications were examined per tested substance.

Chemotropism percentages were calculated as ratio of germtubes showing a detectable positive chemotropic response per number of all germtubes with distinct growth direction

in relation to the filter disc. Three or more biological replications were examined per tested substance.

Values were statistically treated (mean ± standard deviation) and tested for significant differences using ANOVA (InfoStat, version 2016e, InfoStat Group, University of Córdoba, Argentina). Effects were considered significant if $p < 0.05$ in the Tukey test. Graphs were prepared with SigmaPlot 12.5 (Systat Software Inc.).

1. 3 Results

Several plant oils, including native sunflower oil, were tested for their capacity to induce germination of *O. cumana* and *P. ramosa* (Fig. 1.1), because recent investigations have shown that sunflower seeds contain STL (Meier 2018). In the germination bioassay, 20 µl of undiluted sunflower oil had a similar effect as GR24 (1 ppm) on *O. cumana*, whereas mineral oil, olive oil and rape seed oil did not induce germination.

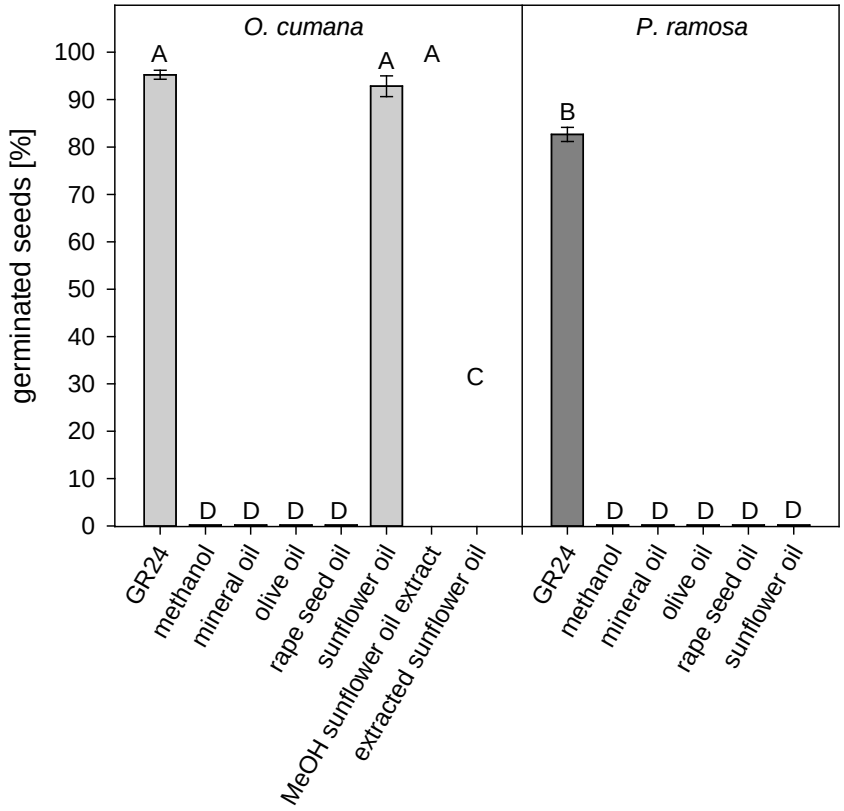

Fig. 1.1 Germination percentages of *O. cumana* and *P. ramosa* seeds in response to plant seed oils, as well as a methanolic (MeOH) sunflower oil extract, the remaining extracted sunflower oil, the artificial strigolactone GR24 (positive control) and methanol (negative control). Every substance was tested in replications of n=3 (except sunflower oil with n=6). The same letter indicates that differences are not statistically significant (Tukey test, $p < 0.05$).

The stimulating agents in sunflower oil could be extracted with methanol and were identified as costunolide, dehydrocostuslactone, 8-epixanthatin and tomentosin by means of HPLC-MS measurements (data not shown, Meier 2018). The methanolic extract induced high germination percentages similar to the unextracted oil, whereas the extracted oil induced less germination (Fig. 1.1). The STL costunolide and dehydrocostus lactone also induced germination (data not shown). Costunolide induced higher germination percentages, so this compound was chosen as STL reference for the chemotropism experiments. The germination inducing effect of sunflower oil did not extend to the related parasitic plant *P. ramosa*, which showed high germination percentages in response to the artificial strigolactone GR24, but did not germinate in the presence of sunflower, olive or rape seed oil (Fig. 1.1).

A special bioassay allowed to assess if a substance induced chemotropism of *O. cumana* germtubes (Fig. 1.2). In a Petri dish with water agar, seeds were placed in a circle around a filter disc containing the tested substance, allowing the substance to diffuse into the agar (Fig. 1.2 a, b).

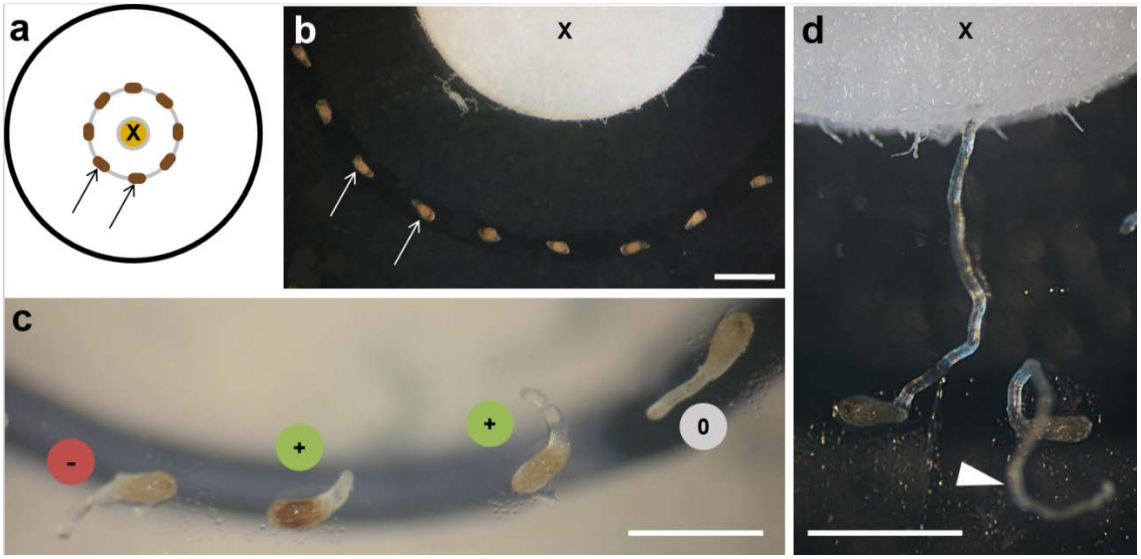

Fig. 1.2 *O. cumana* germtubes in the chemotropism bioassay. **a** Schematics of the chemotropism bioassay. The tested substance was applied onto a filter disc (*X*) and seeds (*arrows*) were placed in a circle 2 mm away from the filter. **b** Chemotropism bioassay setup: seeds (*arrows*) were placed in a circle around the filter containing the tested substance (*X*) with their micropyle facing alternatively left and right. **c** Germtubes in a chemotropism bioassay bending either towards the substance source (+), away from it (-) or showing no distinct reaction (*0*). **d** Detail of two germtubes, one touching the filter with the tested substance (*X*), the other growing away from the substrate (*arrowhead*). *Scale bars* = 1 mm.

After 3–5 days, the seeds started to germinate and the direction of the germtube tip was recorded. The hyaline germtubes of *O. cumana* had a conical tip that became more rounded over time and appeared often more opaque under the dissecting microscope (Fig. 1.2 c). If the germtube bended towards the substance source, it was considered showing positive chemotropism (+), negative chemotropism if it grew away from it (-) or no distinct reaction (0; Fig. 1.2 c, d). Germtubes were approximately 100 µm in diameter and could grow up to 2–3 mm long (Fig. 1.2 d). Chemotropism (either positive or negative) could be evaluated in 35±17 % of all seeds or 70±17 % of germinated seeds (n=39 samples).

More than the half of the germtubes grew upwards away from the substrate (Fid. 1.2 d, arrowhead) in the chemotropism bioassays (61±13 % with costunolide as germination stimulant and 57±17 % with GR24). Therefore, the influence of gravity was tested. When agar plates with the seeds were placed bottom-up (the seeds did not fall off due to adhesion) again 68±10 % (costunolide) and 61±8 % (GR24) of the emerged germtubes grew away from the substrate (in this case, down). There were no significant differences in percentages of germtubes growing away from the substrate, no matter what their orientation in relation to gravity was (Fig. 1.3).

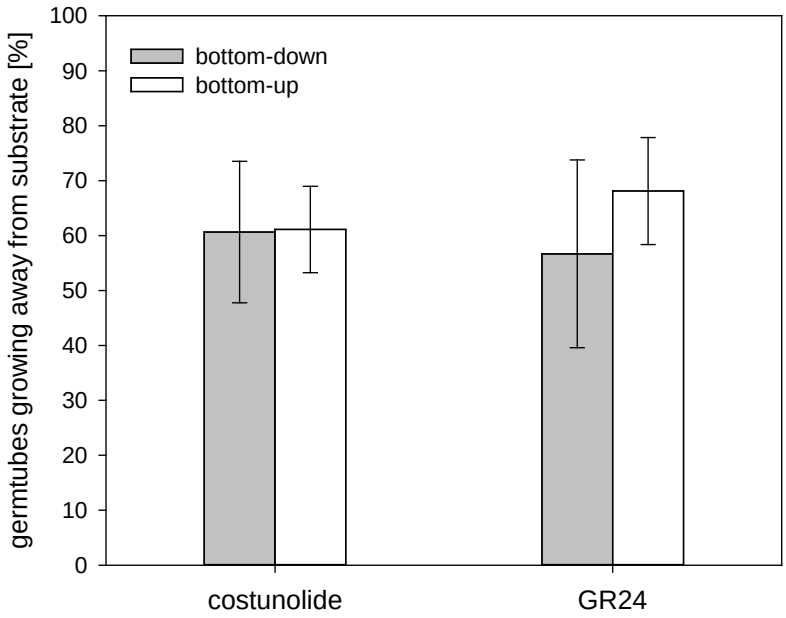

Fig. 1.3 Orientation of *O. cumana* germtubes in relation to gravity. Percentage of germtubes growing away from the substrate if the Petri dish was either placed bottom-down (n=5 per substance) or bottom-up (n=2 per substance). In both cases, and with both the STL costunolide (10^{-4} M) and the strigolactone GR24 (3.3×10^{-6} M), around 60 % of the germtubes grew away from the substrate and showed no gravitropism. Percentages are means ± standard deviation. No significant differences between the two treatments were found with the Tukey test ($p < 0.05$).

In the root chamber system that allowed monitoring of the parasite's underground life stages the growth direction of *O. cumana* germtubes in relation to the host roots was recorded (Fig. 1.4). 75±5 % of the germtubes grew towards the host roots. In chemotropism bioassays, sunflower root exudate, sunflower oil extract and costunolide (10^{-4} M) induced high levels of positive chemotropism. GR24, an artificial strigolactone that induces germination of many root parasitic plants, did not induce chemotropism at a concentration of 3.3×10^{-6} M (1 ppm; Fig. 1.4).

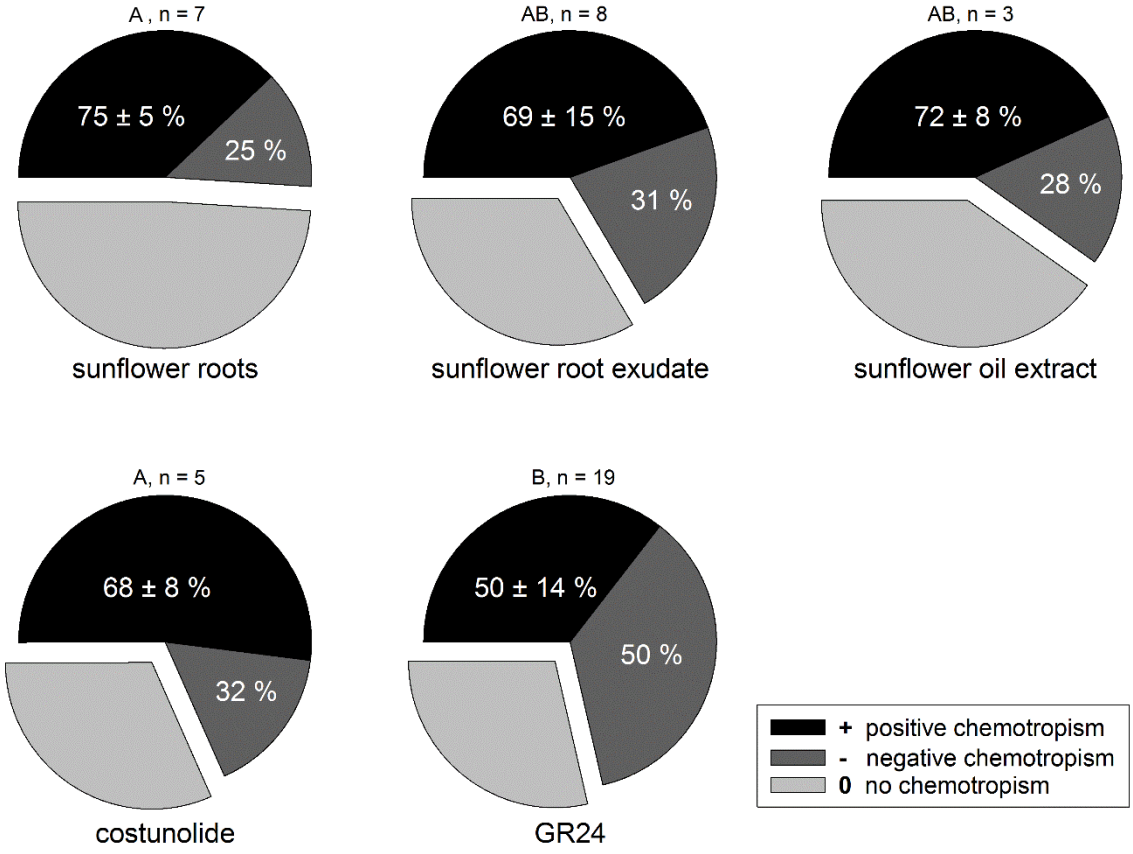

Fig. 1.4 Chemotropism of *O. cumana* germtubes towards sunflower roots in root chamber experiments and towards test substances in chemotropism bioassays with sunflower root exudate, sunflower oil extract, costunolide (10^{-4} M) and GR24 (3.3×10^{-6} M) as substance sources. Percentage of positively (*black*) and negatively (*dark grey*) chemotropic germtubes are given in the pie charts, considering only the germtubes with a clear growth direction. The germtubes that could not be evaluated because they did not show clear tropism (*light grey*) were not included in the calculation. Percentages are means ± standard deviation of several biological replications (*n*). The same letter indicates that differences are not statistically significant (Tukey test, $p < 0.05$).

The ability to induce positive chemotropism depended on the substance concentration (Fig. 1.5). When costunolide was applied at a concentration of 10^{-7} M or 10^{-6} M, only 55±13 % and 56±12 % of germtubes, respectively, showed positive chemotropism. At 10^{-5} M, however, costunolide caused 68±8 % of germtubes to grow towards the substance source and the value raised to 76±17 % at 10^{-4} M.

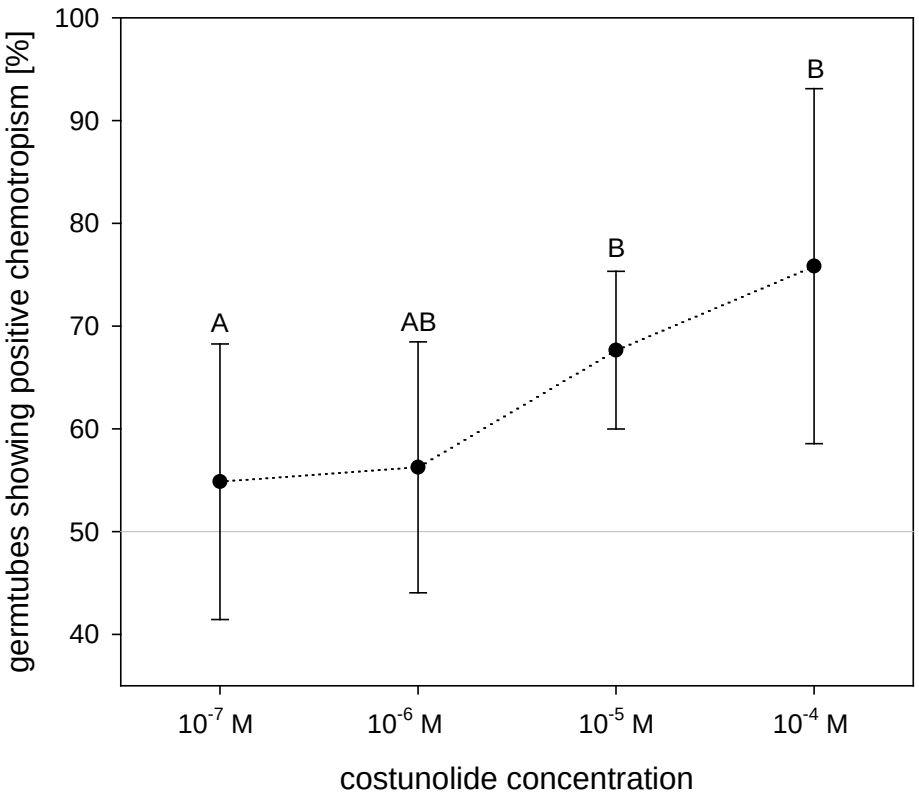

Fig. 1.5 Concentration dependence of *O. cumana* chemotropism towards costunolide. At higher concentrations, chemotropism was significantly higher. Means ± standard deviation of n=3–6 replications. The same letter indicates that differences are not statistically significant (Tukey test, $p < 0.05$).

The ability to induce positive chemotropism was also depending on the distance from the substance source (Fig. 1.6). Within 2 mm of the substance source, 76±17 % of germtubes grew towards costunolide (10^{-4} M), while in the outer zone (2–5 mm), only 48±11 % showed positive chemotropism. For GR24 no significant difference in relation to distance was detected.

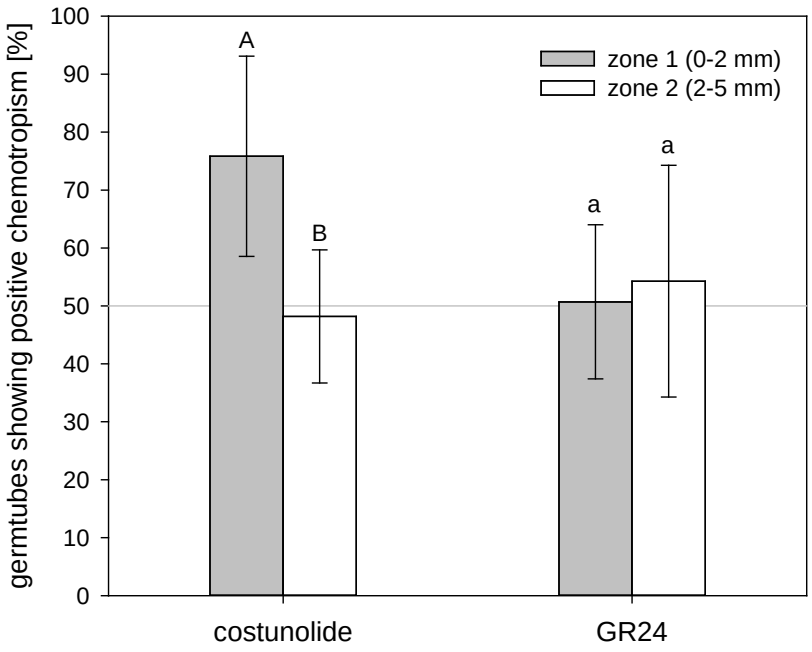

Fig. 1.6 Distance dependence of *O. cumana* chemotropism towards costunolide in contrast to GR24. Germtubes closer to the substance source showed significantly higher chemotropism percentages towards costunolide (10^{-4} M), but not towards GR24 (3.3×10^{-6} M). Means ± standard deviation of n=5–7 replications. The same letter (capitals for costunolide and lower-case for GR24) indicates that differences are not statistically significant (Tukey test, $p < 0.05$).

1. 4 Discussion

Germination and chemotropism bioassays confirmed the bioactivity of sunflower STL on *O. cumana* germination and showed that they play an important role in chemotropism.

Germination of *O. cumana* was induced by sunflower seed oil which contained STL that could be extracted with methanol. These seed STL might not play a role for *O. cumana* under field conditions as long as the sunflower seeds are not damaged. However, with the beginning of sunflower germination and the decrease in concentration of the compounds in cotyledons (Schmauder 2015), they could be exudated by the growing radicle into the soil. Sunflower seed oil was not known yet as germination stimulant for *O. cumana*. It may be used as a cheap and easily available source for positive controls in *O. cumana* germination tests. Sunflower oil did not induce germination of *P. ramosa*. This is in contrast to sunflower root exudates which did induce *P. ramosa* germination (Fernández-Aparicio *et al.* 2009) and suggests that the oil did not contain heliolactone, a strigolactone

found in sunflower root exudates particularly after phosphorous or nitrogen starving (Ueno *et al.* 2014).

Chemotropism of about 70 % of the *O. cumana* germtubes was induced by sunflower root exudate, seed oil extract and the STL reference costunolide, thus corroborating the potential role of STL as signalling compounds for growth direction. The effect of costunolide depended on its concentration. This coincided with the decrease of chemotropic reaction with increasing distance between substance source and seeds which is due to diffusional effects. A gradient in STL concentration also could explain the mechanism behind the curvature of germtubes. Sunflower STL have been reported to inhibit auxin-induced elongation growth (Spring & Hager 1981) and 8-epixanthatin was found to cause curvature of sunflower hypocotyls when applied unilaterally (Yokotani-Tomita *et al.* 1999). The latter could recently be shown for costunolide as well and seems to be a general feature of α,β-unsaturated-γ-lactones (Smith 2018; O. Spring, personal communication). Hence, a difference in concentration of STL between the host-facing and the opposite flank of the *O. cumana* germtube could cause a curvature towards the host. This hypothesis could be tested in the future by examining the anatomy of curved germtubes and recording the cell number and size of their flanks.

It was interesting that GR24 did not have a chemotropism-inducing effect. This could be either because the concentration was high enough to induce germination, but too low to induce chemotropism, or because GR24 does not have a chemotropism-inducing effect on *O. cumana* germtubes. It would be interesting to test the natural strigolactones that induce germination of other parasitic plants for an additional chemotropism-inducing effect. GR24 has been shown to stimulate primary root growth in *Arabidopsis thaliana* (L.) HEYNH. (Ruyter-Spira *et al.* 2011) and it is suspected that such strigolactones play a general role in plant seed germination (Yoneyama *et al.* 2013). The different biological function of strigolacones in contrast to STL might explain their difference in chemotropism-inducing capacity for *O. cumana*. It remains to be elucidated which plant natural compounds induce chemotropism in other Orobanchaceae species and if the STL that only induce germination of *O. cumana* but not of other parasitic plants could still have an effect on thegermtubes of other species.

Some of the *O. cumana* germtubes did not exhibit a chemotropic response. This has also been observed in *Striga* chemotropism (Williams 1961) and in *O. crenata* (Whitney &

Carsten 1981). It is possible that the tip of the *O. cumana* germtube, which consists of smaller cells with dense cytoplasm and large nuclei (Losner-Goshen *et al.* 1991, Joel & Losner-Goshen 1994), can also perceive other external stimuli and respond accordingly, analogously to root tips. Gravitropism does not seem to play a role (Losner-Goshen *et al.* 1991, Joel & Losner-Goshen 1994), but it is possible that the germtubes grow towards oxygen, a process called aerotropism or oxytropism (Porterfield & Musgrave 1998), which would also explain that ca. 60 % of the germtubes grew away from the substrate. If hydrotropism plays a role remains to be elucidated.

Chapter 2: Development of *O. cumana* on susceptible and resistant sunflowers

Some of the results presented in this chapter (namely those that are presented here in Fig. 2.3 and Fig. 2.5) are part of the M.Sc. thesis of Patrizia Gurrata (2016) conducted under my co-supervision.

2. 1 Introduction

Resistance is the ability of an organism to withstand unfavourable conditions. In plants this can be initiated by abiotic stresses such as drought, or biotic stresses like pathogens. Resistance of host plants to root parasitic plants is often complex and seldom an all-or-nothing process. The behaviour of a host plant towards a parasitic plant can be susceptible, tolerant or resistant. On susceptible hosts, the parasite can thrive and complete its lifecycle, the interaction is compatible. Tolerance describes the phenomenon when the parasite develops well, yet growth of the host is less affected than might be expected with the amount of parasites present (ter Borg 1986) or there is no significant yield loss (Wegmann *et al.* 1991). A resistant host has the ability to avoid or withstand parasite attack in a manner that prevents parasite establishment and growth (Timko & Scholes 2013), so that the interaction is incompatible. Resistance mechanisms against root parasites of the Orobanchaceae can act on different developmental stages of the parasite. Pre-attachment resistance mechanisms comprise all mechanisms that allow the host to avoid or prevent attachment (Timko & Scholes 2013). This includes processes that reduce the chance of contact between parasite and host, such as a lack of germination stimulants or deep growing roots, and is also called avoidance (ter Borg 1986). Post-attachment resistance mechanisms occur once the haustorium has formed and the parasite attempts to penetrate host root tissues and to connect to the host's vascular tissue (Timko & Scholes 2013). This 'true resistance' occurs when the parasite is unable to penetrate the host or its growth is greatly reduced (ter Borg 1986). There are several phases at which post-attachment resistance mechanisms can act (Yoshida & Shirasu 2009). Mechanisms acting from the first contact with the host root until establishment of the vascular connection are called pre-haustorial, i.e. before a functional haustorium is formed (Pérez-de-Luque *et al.* 2009). Nevertheless, the structure of the parasite connecting to and penetrating into the host root is usually called haustorium (Joel 2013), regardless of its

functionality, so this term can be confusing. Post-haustorial mechanisms act once vascular connections are formed and the haustorium is functional (Pérez-de-Luque *et al.* 2009).

For *O. cumana*, the currently most severe parasitic threat for sunflower cultivation in S- and E-Europe as well as N-Africa and Asia, all three types of interaction with host genotypes have been observed, e.g. in a field experiment in Spain (Fig. 2.1). Susceptible plants mostly survive, but severely suffer from water and nutrition depletion through the parasite compared to resistant plants in the same environment (Fig. 2.1 a). Interestingly, tolerant plants can show nearly no developmental symptoms and yield loss, although their root system is heavily infested by broomrape (Fig. 2.1 b).

Fig. 2.1 Interaction types of sunflower with *O. cumana* in a field experiment near Sevilla (Spain). **a** Resistant (left row and background) and susceptible (row 2–5 from the left) sunflower genotypes. Susceptible sunflowers are heavily infested with *O. cumana* (*arrows* point to flowering shoots, often 20–50 per host plant), so that they are poorly developed and show signs of wilting. **b** Tolerant sunflower genotype with attached *O. cumana* plants in flowering stage (*arrows*). Infested host plants were well developed and did not differ in height or biomass from uninfested plants.

Resistance of sunflower against *O. cumana* was first observed in Russia in the early 20th century (for references see Škorić *et al.* 2010, Antonova 2014). It is originally based on single dominant genes following the gene-for-gene interaction (reviewed by Fernández-Martínez *et al.* 2015, Velasco *et al.* 2016). However, the use of single dominant genes in

sunflower breeding poses a great evolutionary pressure on *O. cumana* populations to overcome this resistance. Over decades of breeding, at least eight different physiological races, or so-called pathotypes ('pathotype' defined according to Spring *et al.* 2018), have developed (Antonova 2014, Fernández-Martínez *et al.* 2015). Since the gene-for-gene-model does not seem to capture the complexity of *O. cumana* pathotypes anymore, a 3-digit-code was proposed to describe the virulence of an *O. cumana* population (Molinero-Ruiz *et al.* 2015).

Despite intensive research on the genetics of sunflower resistance to *O. cumana* and efforts to locate the *Or* genes for molecular marker-assisted breeding, little is known about the resistance mechanism elicited by these genes (Pérez-Vich *et al.* 2013, Fernández-Martínez *et al.* 2015). This accounts even more for the mechanisms which regulate the interaction of tolerant sunflower genotypes with *O. cumana*. However, successful breeding requires knowledge on the biological mechanisms underlying tolerance and resistance in the *O. cumana*-sunflower-system. This is why the early stages of *O. cumana* development on susceptible, resistant and putatively tolerant hosts were compared. The used sunflower genotype T35001, an experimental hybrid provided by an international breeding company, was selected because of its tolerance behaviour for broomrape observed in field trials in Sevilla, Spain (Fig. 2.1 b). In our laboratory experiments, however, we did not observe tolerance reactions and, therefore, this genotype is here addressed as resistant.

2. 2 Material and methods

Plant material and cultivation

Sunflower plants were cultivated in a hydroponic root chamber system together with surface sterilised seeds of *O. cumana* (for details see chapter 3, p. 48 and Fig. 3.1, p. 49). Seven sunflower genotypes with different degrees of resistance were tested: *Helianthus annuus* HA300, 'Giganteus', L7, OR3, OR4, and OR5 (the latter four were generously provided by D. Miladinovic, Novi Sad, Serbia), which were expected to be susceptible to the used *O. cumana* pathotype G (collected in Russia in 2012), and hybrid T35001 (gratefully provided by L. Hargitay, Hungary), which should be resistant. Five root chambers were prepared per sunflower genotype to monitor the development of the parasite. The root chambers were checked weekly under a dissecting microscope for a

month. The total number of seeds per root chamber was counted, as well as the number of germinated seeds, attached seedlings, and tubercles. Additional root chambers were prepared to take samples for microscopy.

To validate the observations on the development of the resistant sunflower genotype T35001 in comparison to the susceptible HA300, five independent root chamber experiments were performed with three *O. cumana* pathotypes: pathotype D (collected in China in 2013, generously provided by D. Ma), pathotype E+ (collected in Spain 2014 by O. Spring), and pathotype G (collected in Russia in 2012, generously provided by Dr. T. Antonova and PhD S. Guchetl). For each host-parasite-combination, 4–11 root chambers were evaluated.

Host (HA300 and T35001) and parasite (pathotypes E+ and G) were grown in pots (10 cm × 10 cm) in an earth-sand-mixture to observe the later stages of broomrape development. The plants were either uprooted to count tubercle numbers or they were cultivated for two months until shoots of *O. cumana* emerged. Five sunflower plants were grown per host-parasite-combination. The pot experiment was repeated twice.

Seed vitality test

The vitality of the *O. cumana* seeds was tested with triphenyl tetrazolium chloride (TTC, method adapted from Thorogood *et al.* 2009). Surface sterilised seeds were spread on Whatman glass fiber filters (diameter 1 cm) and placed in a Petri dish. 300 µl of a 1 % aqueous TTC solution (Fluka Chemie AG, Buchs, Switzerland) were added to the seeds on each Whatman filter and the Petri dishes were sealed with parafilm and wrapped in aluminium foil to stay moist and dark. The samples were incubated for 7 d at 35–37°C. The testa of the seeds was then bleached with sodium hypochlorite (12 %) for 20–30 min, until the inner tissues of the seeds were visible. After rinsing the seeds with water, each Whatman filter was placed onto a glass slide and examined under the microscope. Seeds with reddish contents were considered vital, whereas seeds with yellow content were considered dead. Per seed sample, at least 150 seeds were evaluated.

Calculation of germination, attachment and tubercle percentages and statistics

Germination percentages of the seeds in each root chamber were calculated by dividing the number of germinated seeds by the number of vital seeds (total seed number corrected to the number of vital seeds as determined by the TTC test). Attachment percentages were

calculated as the number of attached seedlings divided by the number of germinated seeds. Tubercle percentages were given as percentages of attached seedlings. The obtained values were statistically treated (mean value, standard deviation). Graphs were prepared using Sigma Plot 12.5 (Systat Software Inc.). Analysis of variance (ANOVA) was conducted on the germination, attachment and tubercle percentages with InfoStat (Version 2016e, InfoStat Group, University of Córdoba, Argentina). Effects were considered significant if $p < 0.05$ in the Tukey test.

Microscopy

To compare the interaction of resistant (T35001) and susceptible (HA300) sunflower genotypes with *O. cumana* pathotype G, samples were prepared for light- and transmission electron microscopy (TEM). Samples of early interaction stages between host and parasite were taken from root chambers after 9, 11, 14 and 21 days post inoculation (dpi). 1–3 mm long pieces of sunflower root with attached *O. cumana*-seedlings were dissected and prepared for light- and transmission electron microscopy as described in chapter 3 (p. 46). Complete longitudinal serial sections of the infected roots and attached *O. cumana* seedlings were prepared. Twelve samples were examined for T35001 and eight samples for HA300.

Additionally, at 14 dpi, fresh whole mount samples of *O. cumana* seedlings attached to the host root were examined by fluorescence microscopy (Zeiss filter 05, 395 nm / 440 nm, Zeiss, Göttingen, Germany). A staining with resorcin blue (Chroma, Münster, Germany) was performed to detect callose. Three samples per host-parasite-combination were examined.

2. 3 Results

Resistance reactions of sunflower against the root parasite *O. cumana* may occur at each of the early underground developmental stages of the parasite, as schematically illustrated in Fig. 2.2. This starts with the absence of induced germination (Fig. 2.2 a), continues with missing chemotropic signals (Fig. 2.2 b), prevention of attachment (Fig. 2.2 c), inhibition of penetration / haustorium formation (Fig. 2.2 d) and connection to the vascular bundle (Fig. 2.2 e), and ends with the suppression of tubercle formation or necrosis of the tubercle (Fig. 2.2 f).

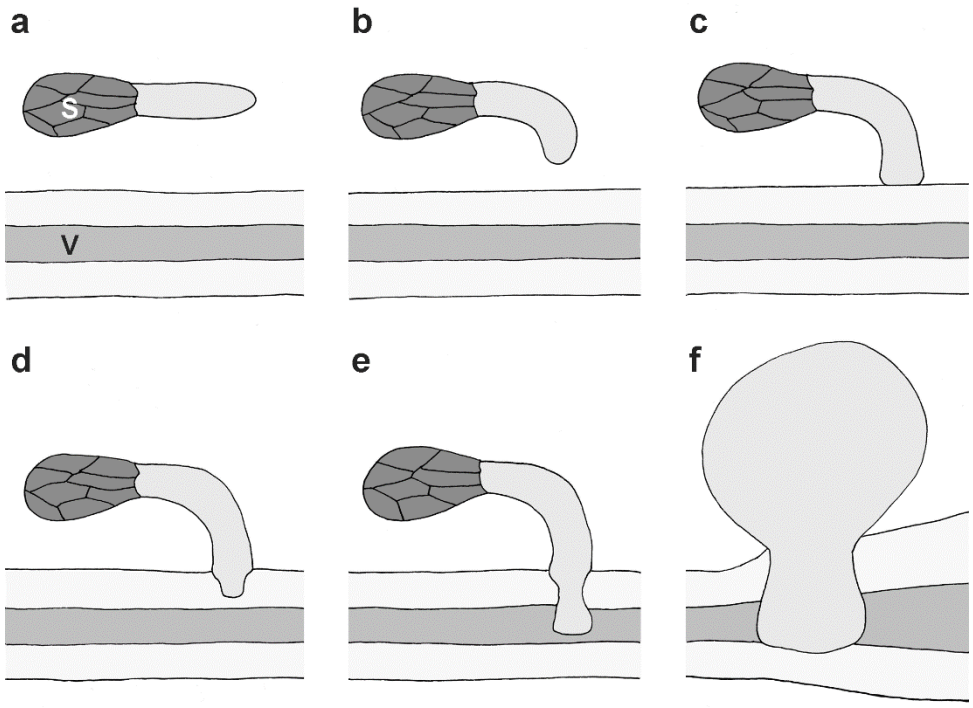

Fig. 2.2 Diagram of the developmental stages of *O. cumana* where host resistance mechanisms can act to hinder further parasite development: **a** germination, **b** chemotropism, **c** attachment, **d** penetration, **e** vascular connection, **f** tubercle formation. *S* = *O. cumana* seed, *V* = vascular bundle of the host root, depicted in longitudinal section.

To observe at which of these stages resistance occurs, *O. cumana* development was monitored on seven host genotypes, including L7, OR3, OR4, OR5, HA300 and *H.annuus* 'Giganteus', which were susceptible to the used *O. cumana* pathotype G, and T35001, which was resistant.

O. cumana germinated with all tested sunflower genotypes (Fig. 2.3 a). After one week, seeds had germinated in every root chamber. Seeds continued to germinate during the second week. When the final germination percentages were compared, there were significant differences, although standard deviation was high for all tested genotypes (table 2.1, error bars for the percentages are not shown in Fig. 2.3 due to clarity, but for the counts given on the right). In five biological replicates, T35001 induced a comparatively low germination percentage of 37±23 %, but there was high variation within the five root chambers. To verify if T35001 always induces a lower germination than the susceptible sunflowers, this experiment was repeated several times with T35001 and HA300 as a susceptible control. Again, there was high variation, with germination percentages of 54±26 % in root chambers with T35001 (n=19) and 65±22 % for HA300 (n=12).

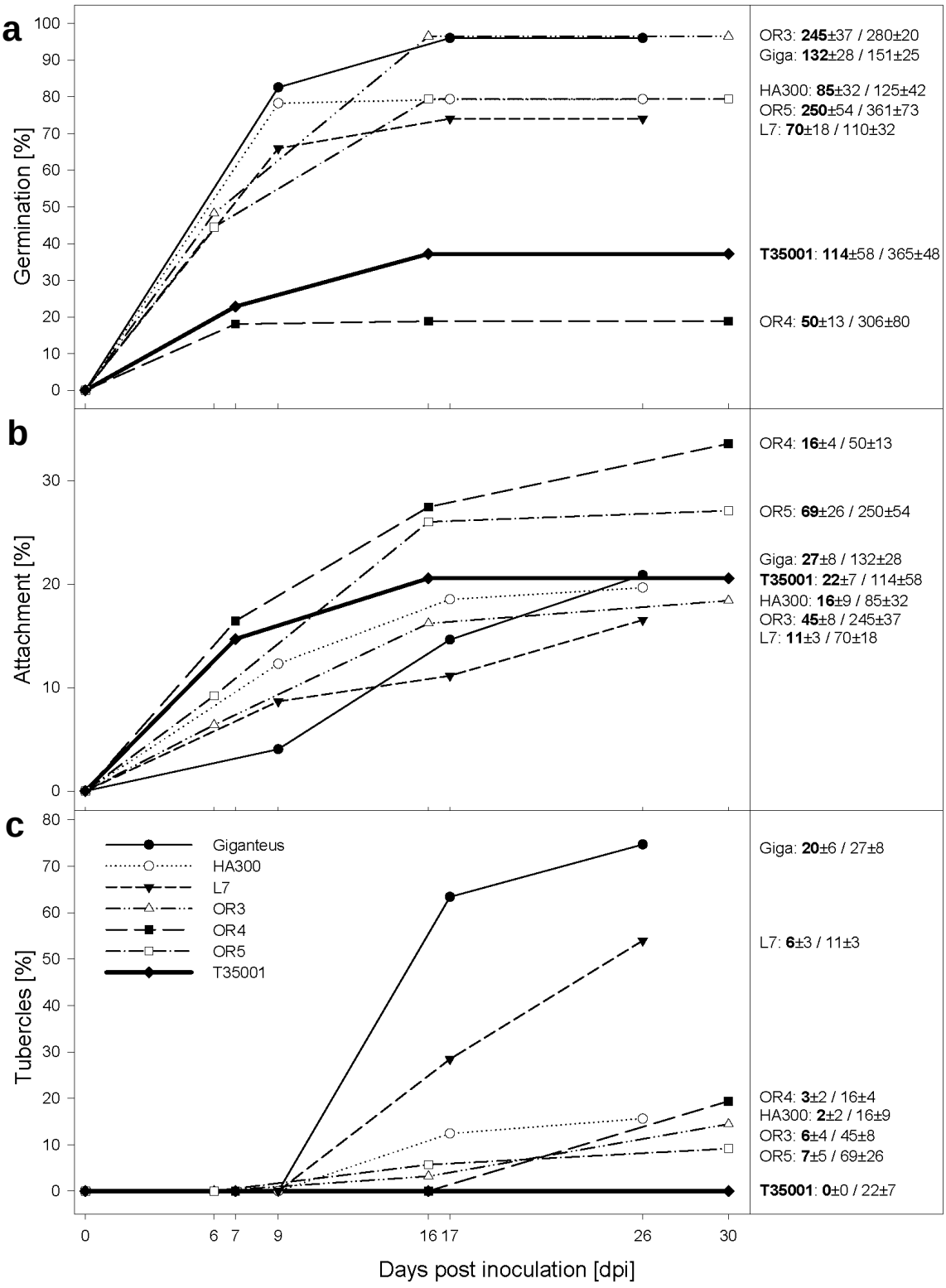

Fig. 2.3 Development of *O. cumana* pathotype G with susceptible and resistant host genotypes. All sunflowers tested were susceptible, except the resistant T35001. **a** germination, **b** attachment, **c** tubercle percentages. Numbers indicate the mean value ± standard deviation of the total numbers counted in the root chambers (n=5 root chambers per genotype, except L7 with n=4). Germination percentages were corrected for the amount of vital seeds (87.5 %). Attachment percentages were calculated as number of attached *O. cumana* seedlings per number of germinated seeds. Tubercle percentages are given as number of tubercles per number of attached seedlings.

Table 2.1 Germination (*germ*), attachment (appressoria, *app*) and tubercle (*tub*) percentages of seven sunflower genotypes in root chambers with *O. cumana* pathotype G. Mean value (⌀) and standard deviation (*SD*) of n=5 root chambers per genotype (n=4 for L7) at three points in time post inoculation (*dpi*). Germination percentages were corrected for the amount of vital seeds (87.5 %). Attachment percentages = attached seedlings / germinated seeds, tubercle percentages = tubercles / attached seedlings. An ANOVA was performed with the values at the final dpi. The same letter indicates that differences are not statistically significant (Tukey test, $p < 0.05$)

genotype		dpi	germ	app	tub	dpi	germ	app	tub	dpi	germ	app	tub
L7 (-OR)	**⌀**	**9**	66	9	0	**17**	74	11	28	**26**	74 ^{C}	17 ^{A}	54 ^{C}
	SD		14.15	3.06	0		11.49	4.14	19.35		11.49	4.10	8.17
OR3	**⌀**	**6**	48	6	0	**16**	99	16	3	**30**	99 ^{D}	18 ^{AB}	14 ^{B}
	SD		11.24	4.00	0		9.00	3.03	1.42		9.00	3.26	8.82
OR4	**⌀**	**7**	18	16	0	**16**	19	27	0	**30**	19 ^{A}	34 ^{C}	19 ^{B}
	SD		4.25	5.47	0		3.43	10.15	0		3.43	10.27	8.24
OR5	**⌀**	**6**	45	9	0	**16**	79	26	6	**30**	79 ^{CD}	27 ^{BC}	9 ^{AB}
	SD		7.06	5.16	0		10.79	5.55	3.62		10.79	6.35	3.39
HA300	**⌀**	**9**	78	12	0	**17**	79	19	12	**26**	79 ^{CD}	20 ^{AB}	16 ^{B}
	SD		22.74	2.92	0		20.35	8.89	15.33		20.35	10.41	15.87
Giganteus	**⌀**	**9**	84	4	0	**17**	99	15	63	**26**	99 ^{D}	21 ^{AB}	75 ^{D}
	SD		17.48	2.94	0		8.49	5.44	9.10		8.49	6.70	5.42
T35001	**⌀**	**7**	23	15	0	**16**	37	21	0	**30**	37 ^{B}	21 ^{AB}	0 ^{A}
	SD		9.73	8.12	0		22.88	5.17	0		22.88	5.17	0

There was no significant difference between the germination percentages of *O. cumana* pathotype G with T35001 or HA300. This was confirmed in repetitions with the *O. cumana* genotypes D and E+, where germination also occurred in every root chamber, regardless if the host was the resistant T35001 or the susceptible HA300 (data not shown).

After germination, the attachment of *O. cumana* seedlings to the host roots was monitored. Some seedlings had already attached to the host root after one week, but the highest attachment percentages were observed after four weeks (Fig. 2.3 b). The final attachment percentages ranged from 17±4 % (L7) to 34±10 % (OR4). Seedlings in root chambers with T35001 showed an average value of 21±5 %, similar to the susceptible genotypes HA300 and 'Giganteus'. Closer examination under a dissecting microscope revealed that the seedlings did not only touch the host roots by accident, but formed appressoria (as schematically illustrated in Fig. 2.2 c). A reddish layer was sometimes visible at the contact point between appressorium and root (e.g. Fig. 2.5), regardless of the host genotype. All in all, no difference between the resistant T35001 and the susceptible hosts was observed at the appressorium stage.

However, a significant difference was observed at the tubercle stage (Fig. 2.2 f). While 9±3 % (OR5) to 75±5 % ('Giganteus') of the appressoria developed into tubercles on the susceptible sunflower genotypes, no tubercles were found on the resistant sunflower genotype T35001 at all (Fig. 2.3 c). This was also observed in a repetition of the experiment with the *O. cumana* pathotypes D and E+ on HA300 and T35001 roots. While both pathotypes formed tubercles on HA300 roots, no tubercles were ever observed on T35001.

The pot experiments that were conducted to confirm these unexpected observations from the root chambers with T35001 showed the same result (Fig. 2.4). The *O. cumana* pathotypes E+ and G formed no tubercles and shoots with T35001 (Fig. 2.4 c), whereas there were ca. 5–10 tubercles per plant in the interaction with HA300 (Fig. 2.4 a, b).

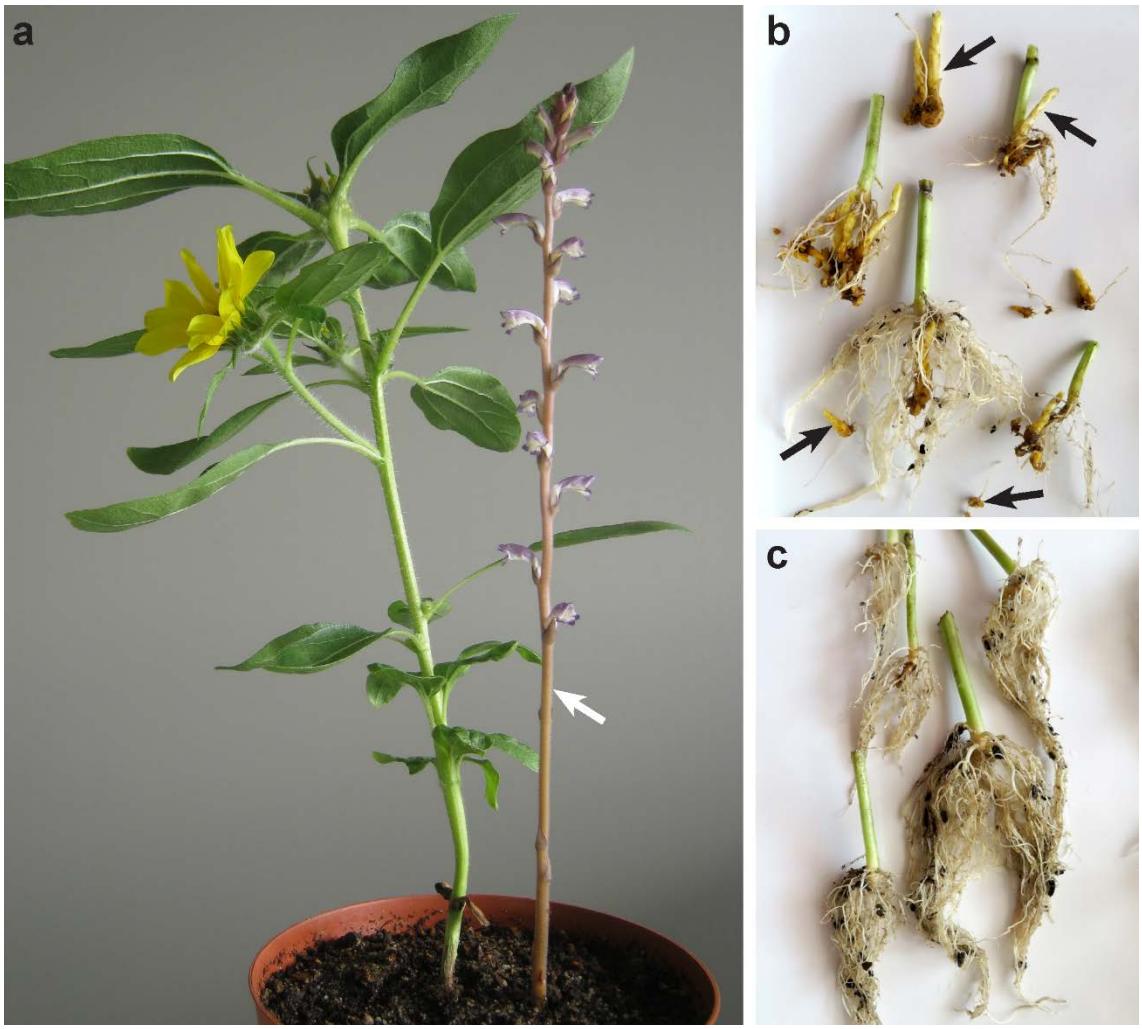

Fig. 2.4 Development of tubercles in pot experiments. **a** Shoot (*arrow*) of *O. cumana* pathotype G on the susceptible host HA300, **b** tubercles (*arrows*) on the roots of HA300, **c** root system of the resistant sunflower genotype T35001 without tubercles.

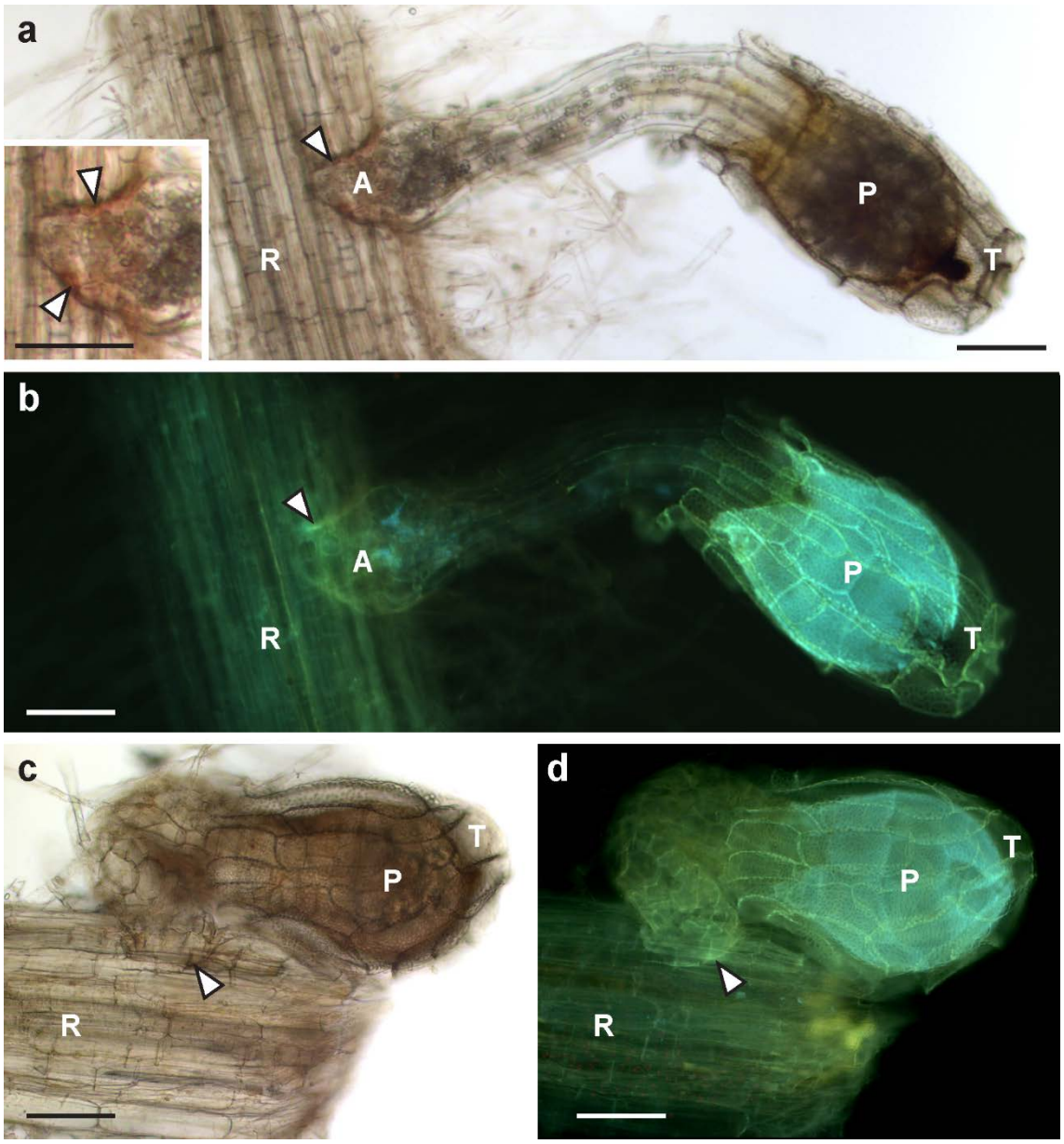

Fig. 2.5 Light microscopy of *O. cumana* seedlings on susceptible and resistant hosts 14 dpi, whole mounts investigated by bright field (a, c) and fluorescence microscopy (b, d), identical sites, respectively. **a** appressorium (*A*) on a susceptible HA300 host root (*R*), *inset*: the margin of the appressorium shows a reddish staining (*arrowheads*); dark perisperm (*P*) under the testa (*T*), **b** intense autofluorescence of the margin of the appressorium (*arrowhead*) as well as of the testa (*T*) and perisperm (*P*); host root (*R*), appressorium (*A*). **c** Appressorium (*arrowhead*) on a resistant T35001 host root (*R*); dark perisperm (*P*) under the testa (*T*). **d** autofluorescence of the margin of the appressorium (*arrowhead*) as well as of the testa (*T*) and perisperm (*P*); host root (*R*). *scale bars* = 100 µm.

Samples were prepared for microscopy to elucidate why *O. cumana* could not form tubercles on roots of the resistant genotype T35001. Whole mount samples of young *O. cumana* seedlings attached to susceptible and resistant hosts were compared (Fig. 2.5). The seedling emerged as a hyaline germ tube from the seed coat (testa) and attached to the host root with an appressorium. The margin of the appressorium showed a reddish colouring in both susceptible (Fig. 2.5 a) and resistant (Fig. 2.5 c) interactions. This reddish colouring was autofluorescent, similar to the testa and the inner tissues of the seed (perisperm, Fig. 2.5 b, d). No differences were observed between the appressoria of resistant and susceptible interactions. A resorcin blue staining revealed no callose at the penetration site of haustoria in the resistant interaction (data not shown).

The development of haustoria in the susceptible interaction was examined by light microscopy (Fig. 2.6). After penetration of the rhizodermis and cortex (Fig. 2.6 a), the haustorium connected to the vascular tissue of the host (Fig. 2.6 b). After three weeks, small tubercles with extensive connection to the host's vasculature had developed (Fig. 2.6 c).

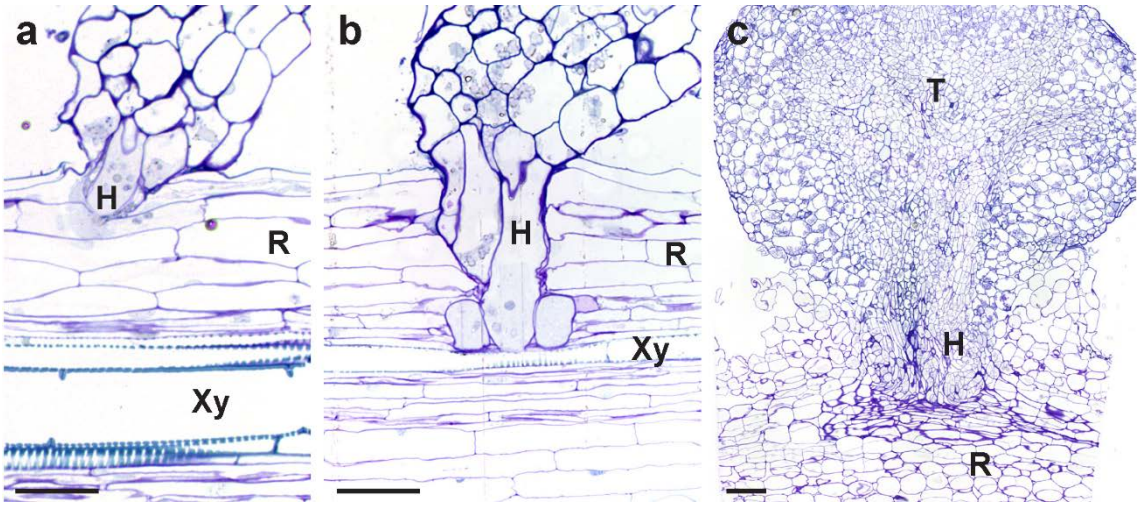

Fig. 2.6 Light micrographs of compatible interactions demonstrating haustoria and a tubercle on a susceptible host root. **a** A haustorium (*H*) penetrating the host root (*R*); 11 dpi, xylem (*Xy*), *scale bar* = 50 µm. **b** A haustorium (*H*) reaching the vascular bundle; 11 dpi, host root (*R*), xylem (*Xy*), *scale bar* = 50 µm. **c** A haustorium has formed a connection to the host vascular bundle and formed a tubercle (*T*); 21 dpi, host root (*R*), *scale bar* = 100 µm. Longitudinal sections, *H. annuus* HA300 with *O. cumana* pathotype G.

In contrast, tubercle formation was never observed on the roots of the resistant sunflower genotype T35001 (Fig. 2.7). Haustoria penetrated the rhizodermis and cortex, but never reached the vascular bundle of the host root (Fig. 2.7 a, b, e). No cytological reactions were observed in the cortex cells within the first phase of penetration. Ultrastructural investigations using transmission electron microscopy revealed no fortifying structures, such as cell wall thickening or callose deposition. Later on, the cortex cells showed signs of degeneration with bacteria inside the cells (Fig. 2.7 c) and ruptured cell walls (Fig. 2.7 f). The haustorial cells also showed signs of degeneration such as inverse contrast in the cytoplasm (Fig. 2.7 f, g).

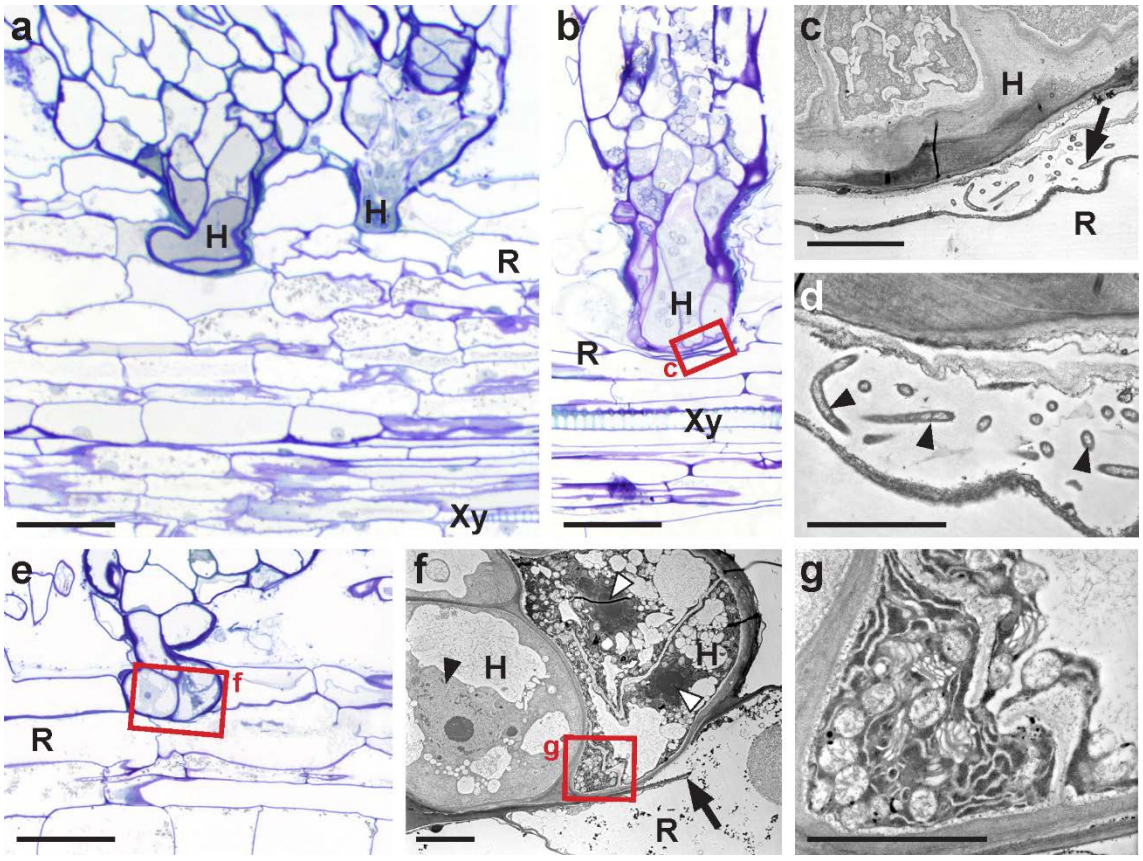

Fig. 2.7 Light- and electron micrographs of incompatible interactions. **a** Two haustoria (*H*) penetrating the cortex of the host root (*R*); 21 dpi, xylem (*Xy*), light micrograph, *scale bar* = 50 µm. **b** A haustorium (*H*) penetrating the cortex but not reaching the xylem (*Xy*) of the host; 9 dpi, host root (*R*), light micrograph, *scale bar* = 50 µm. **c** Transmission electron micrograph of a serial section near *b*. Tip of the haustorium (*H*) in contact with a host root cell (*R*), bacteria were present in the root cortex cell (*arrow*); *scale bar* = 10 µm. **d** Detail of *c*; bacteria (*arrowheads*), *scale bar* = 5 µm. **e** A haustorium penetrating the rhizodermis of the host root (*R*); 21 dpi, light micrograph, *scale bar* = 50 µm. **f** Transmission electron micrograph of a serial section near *e*. Two cells of the haustorium (*H*) showing signs of degeneration with highly contrasted nuclei (*white arrowheads*) and inverse contrast of the cytoplasm; nucleus in vital haustorial cell (*black arrowhead*), broken host root (*R*) cell wall (*arrow*), *scale bar* = 10 µm. **g** Detail of *f*; Degenerated cytoplasm of the haustorial cell showing inverse contrast; *scale bar* = 5 µm. Longitudinal sections, *H. annuus* T35001 with *O. cumana* pathotype G.

2. 4 Discussion

There are several decisive steps that *O. cumana* has to undergo in order to successfully parasitise its host: germination, chemotropism, attachment, penetration, connection to the vascular bundle and tubercle formation (Fig. 2.2). This means that early resistance mechanisms of sunflower can act at each of these steps. The aim of this study was to elucidate at which point of the *O. cumana* life cycle resistance mechanisms of the sunflower genotype T35001 act.

O. cumana germination was induced by all seven sunflower lines tested in this study and no correlation to the resistance or susceptibility of the host was observed. So apparently all tested genotypes produce and exudate the germination stimulants for *O. cumana*. These have been identified as sesquiterpene lactones (STL) that act at very low concentrations (Joel *et al.* 2011, Raupp & Spring 2013). Another germination stimulant that was found in sunflower root exudates is heliolactone (Ueno *et al.* 2014). Broomrape resistance of sunflower due to a lack of exudated germination stimulants has been repeatedly discussed as a goal for sunflower breeding (Wegmann 1986, Pérez-de-Luque *et al.* 2009, Pérez-Vich *et al.* 2013). However, to our knowledge, no such sunflower genotypes have been developed so far. STL play important physiological roles in phototropism and communication in the rhizosphere (as reviewed by Padilla-Gonzalez *et al.* 2016). It is thinkable that STL are so important for sunflower physiology and interaction with the environment, that finding genotypes that do not exudate STL is unlikely.

In the seven studied sunflower genotypes, the amount of exudated STL does not seem to differ significantly, since they all induced germination of *O. cumana* seeds. This is in accordance with studies of M. Schädlich (2013), who determined the amount of the four known germination-inducing STL dehydrocostus lactone, costunolide, 8-epixanthatin and tomentosin in the root exudates of nine sunflower genotypes. Despite some differences in the detected STL, the amounts were sufficient in all root exudates to induce germination of *O. cumana* seeds (Schädlich 2013, Krupp 2014). The independence of germination induction from the susceptibility or resistance of a host was also confirmed in other studies. Dörr *et al.* (1994) and Echevarría-Zomeño *et al.* (2006) observed no significant difference in the germination percentages of a susceptible and a resistant sunflower genotype. Véronési *et al.* (2005) studied germination of four *O. cumana* populations on root exudates of seven sunflower genotypes (totally susceptible and OR1–

OR6). Interestingly, there were no significant differences within the *O. cumana* populations, but within the sunflower genotypes. Nevertheless, all sunflowers induced germination. Labrousse *et al.* (2001) observed differences in the germination dynamics of *O. cumana* seeds induced by root exudates of three sunflower genotypes at different ages. While germination percentages induced by the exudates of the susceptible genotype and one of the two resistant genotypes reached a maximum at week 5, there was a decline for the second genotype after week 2. The maximum germination percentage of the resistant genotypes was lower, but with 35% of the seeds still considerable (Labrousse *et al.* 2001). Evaluation of 90 recombinant inbred lines between a resistant (LR1) and a susceptible (HA89) sunflower parent revealed nine lines whose root exudates did not induce germination (Labrousse *et al.* 2004). However, these results were not obtained from co-cultivation of host and parasite in a root chamber, but using root exudates, which poses the risk of over- or under-concentration of germination stimulants. Over-concentration of germination stimulants, so that they have an inhibiting rather than an inducing effect (Raupp & Spring 2013), or the exudation of compounds toxic to *O. cumana* would be another possibility to avoid germination, but no such phenomenon has been described yet. As in the cited studies, germination was not the limiting factor for resistance in the current study.

After germination, *O. cumana* seedlings need to grow towards the host root for attachment. This is caused by chemotropism (see chapter 1, p. 17) and was poorly understood up to date (Joel & Bar 2013). Comparison of the attachment percentages of *O. cumana* seedlings on the roots of the resistant T35001 with those on the susceptible sunflower roots revealed no striking difference in the conducted experiments. So the ability to find the host root does not seem to be impaired, indicating that the chemotropism inducing compounds are present in susceptible and resistant sunflower genotypes as well.

Attachments have been observed also on other resistant sunflower roots (Dörr *et al.* 1994, Labrousse *et al.* 2001, Echevarría-Zomeño *et al.* 2006). So germination, chemotropism and attachment of *O. cumana* do not seem to be the crucial developmental processes that are targeted by resistance mechanisms (Fig. 2.2 a–c).

The first striking differences between the resistant and susceptible interaction were observed during the haustorium and tubercle formation (Fig. 2.2 d–f). Once the seedling has attached to a resistant host root, it can theoretically be stopped in every tissue of the

root by a pre-haustorial resistance mechanism. A stop at the rhizodermis with no penetration into the root has previously been observed, yet the underlying mechanism has not been unravelled (Krupp 2014). On the resistant host roots, *O. cumana* formed appressoria that were attached to the host root with a layer that sometimes had a reddish colour and showed auto-fluorescence. This phenomenon was observed on susceptible and resistant sunflowers and seems to be a general feature of *O. cumana* appressoria and not a reaction of the host root. A change in the cytology of the rhizodermis was not observed (Krupp 2014). In the resistant sunflower roots of the current study, haustorium formation stopped in the cortex, although typical cytological resistance mechanisms could not be observed. An encapsulation of the haustorium by an isolation layer in the root cortex has been reported for *O. cumana* (Dörr *et al.* 1994, Labrousse *et al.* 2001). Also other cell wall changes have been described to block further intrusion of parasitic cells such as a thickening of the host cell walls by suberization and protein cross-linking (Echevarría-Zomeño *et al.* 2006). However, in this study, the cortex cell walls did not show ultrastructural changes and no isolation layer was formed. Instead, a degeneration of haustorium cells was observed, corresponding to browning and necrosis of the seedling. Bacteria were present in some surrounding host cortex cells, which Dörr *et al.* (1994) also observed in incompatible sunflower-*O. cumana*-interactions. Bacteria are residents of the rhizosphere and may colonise the dead cortex cells, but it seems unlikely that they play an active role in destroying them, especially because they were mainly observed in older samples. Also in the cell walls of *O. cumana* seedlings on susceptible hosts, bacteria have been described (Joel & Losner-Goshen 1994). Nevertheless, the parasitation behaviour was not influenced by the presence of bacteria, as experiments under sterile conditions have shown (Joel & Losner-Goshen 1994, Losner-Goshen *et al.* 1998).

In other root parasitic plants, such as *O. crenata* and *Striga* spp., the endodermis has been reported as an important barrier (Pérez-de-Luque *et al.* 2007, Yoshida & Shirasu 2009). In the sunflower-*O. cumana*-interaction, the cortex seems to play the more important role (Dörr *et al.* 1994, Echevarría-Zomeño *et al.* 2006, Sisou *et al.* 2019).

Resistance reactions have also been reported after the parasite has connected to the vascular tissues (Fig. 2.2 e). Vessel occlusion by callose (Letousy *et al.* 2007) or a gum-like substance (Labrousse *et al.* 2001) were observed, as well as xylem vessel occlusion by lignin, possibly due to peroxidase activities of the parasite (Antonova & ter Borg 1996). Also necrosis of tubercles (Fig. 2 f), i.e. a post-haustorial resistance reaction, has

been described (Labrousse *et al.* 2001, Eizenberg *et al.* 2003a, b), although it is not clear yet why the tubercles die off. However, in the experiments with T35001, the haustorium never reached the vascular bundle and no tubercles were formed at all.

It was unexpected that in the experiments of the current study, the putatively tolerant genotype T35001 showed true resistance. Reasons for this reaction remain unclear. Temperature has been described to affect broomrape resistance in sunflower as well as *O. cumana* virulence (Eizenberg *et al.* 2003a, b). It is possible that at the moderate temperatures in the climate chamber experiments compared to the conditions in the field, *O. cumana* metabolism was not active enough to overcome the resistance mechanisms of T35001.

The pre-haustorial resistance mechanisms observed in this study acted in the root cortex and hindered further penetration of the haustorium towards the host's vascular bundle. There are two theoretical possibilities in which the studied resistant sunflower genotype could stop parasite growth in its cortex: Firstly, by hindering the ability of the parasite to grow further, or secondly, by poisoning the intruding parasite cells.

The first possibility takes into account the complexity of the host-parasite-interaction concerning penetration. Pectolytic enzymes excreted by the parasite dissolve the middle lamellae of host cells and allow the parasite to penetrate into host tissues (Losner-Goshen *et al.* 1998). How the parasite accomplishes this without triggering defence reactions of the host is still unknown, but surely requires a balanced signalling between host and parasite. Once this balance is lost and the parasite is detected by the host, resistance mechanisms such as inhibitors of these pectolytic enzymes can be launched (Véronési *et al.* 2005, Höniges *et al.* 2008). Whether this was the case in the resistance reaction observed in this study remains unclear.

As for the second possibility, parasite cells could be poisoned by a substance that was not detectable by its fluorescence. Phytoalexins such as coumarins (e.g. scopoletin) were described to play a role in resistance reactions of sunflower to *O. cumana* (Serghini *et al.* 2001, Sauerborn *et al.* 2002) and an accumulation of toxic phenolic compounds was observed around the haustorium (Echevarría-Zomeño *et al.* 2006). In this study though, no toxic phenolic compounds were observed by fluorescence microscopy. Necrosis of the intruding parasite cells could also be induced by a toxic peptide similar to the described sunflower defensin HaDef1 (de Zélicourt *et al.* 2007). The sunflower defensin-like

peptide HaDef1 was identified to induce necrosis of *O. cumana* seedling apices (de Zélicourt *et al.* 2007) and over-expression of the encoding gene in the resistant sunflower genotype LR1 was correlated to necrosis of *O. cumana* tubercles (Letousy *et al.* 2007, de Zélicourt *et al.* 2007). Further experiments would be necessary to test the involvement of defensins in the observed resistance reaction.

All in all, the differences in the interaction of T35001 with *O. cumana* compared to previously described incompatible combinations indicate that sunflower resistance to broomrape is based on a wide variety of mechanisms. This makes a broader screening necessary and will require additional techniques such as immuno-histological methods or expression studies with tissues of the host-pathogen-interface.

Chapter 3: Development of the phloem connection between *O. cumana* and its host

The content of this chapter was published in:

Krupp, A., Heller, A. & Spring, O. (**2019**) Development of phloem connection between the parasitic plant *Orobanche cumana* and its host sunflower. Protoplasma 256: 1385–1397

3. 1 Introduction

The most important structure in the early development of Orobanchaceae species is the haustorium, the organ which functions as anatomical and physiological bridge between parasite and host (Attawi 1977, Joel 2013, Yoshida *et al.* 2016). To gain access to the host's water and nutrient supplies, the haustorium needs to connect to the host's vascular tissues, i.e. xylem and phloem. Studying the connection between the vascular systems of haustoria and host roots poses some difficulties since host and parasite tissues are tightly intermingled. New cells are formed not only by the parasite but also by the host and cell shapes often differ from their typical form (Dörr & Kollmann 1974, Dörr 1990, Dörr *et al.* 1994, Joel 2013, Spallek *et al.* 2017). This means that phloem in haustoria can often only be detected by means of transmission electron microscopy (TEM). Another difficulty is the identification of a cell as either belonging to the host or the parasite. This has been achieved in the past with the use of ultrastructural cell markers such as spherical particles in the cytoplasm (Dörr & Kollmann 1974), sieve-element plastids, mitochondria and P-protein (Dörr *et al.* 1979, Dörr & Kollmann 1995). Ultrastructural investigations in haustoria of Orobanchaceae species thus revealed great variation between different species in the mode of phloem connections. Phloem in terminal haustoria of *A. vogelii* was separated by parenchyma from the host phloem (Dörr *et al.* 1979). In lateral haustoria of *P. ramosa*, phloem connection via a plasma-rich contact cell was found (Dörr & Kollmann 1975), whereas fully differentiated sieve elements between *O. crenata* and *Vicia narbonensis* L. were directly symplastically connected via an interspecific sieve plate with open sieve pores (Dörr & Kollmann 1995). Phloem cells in the haustorium of *Phelipanche aegyptiaca* (PERS.) POMEL were shown to retain nuclei (Ekawa & Aoki 2017), while no phloem was detected in terminal haustoria of *Striga hermonthica* (DELILE) BENTH. and *Striga asiatica* (L.) KUNTZE (Ba 1988, Dörr 1997). This variability

in phloem systems of haustoria shows that punctual observations cannot be generalised for all Orobanchaceae species.

In *O. cumana*, light microscopic investigations showed that parasite cells get into close contact with the host phloem (Labrousse *et al.* 2010), but the ultrastructural nature of this contact was not studied. Therefore, to gain a greater understanding of the biology of this economically important parasite, a thorough ultrastructural study of phloem development during haustoria, tubercle and shoot establishment was conducted.

3. 2 Material and methods

Plant material and cultivation

Sunflower, *Helianthus annuus* HA300, was cultivated in a climate chamber at 25°C with a 14 h day / 10 h night illumination cycle. Plants were grown hydroponically in a root chamber system (Fig. 3.1, compare also Pérez-de-Luque *et al.* 2005, Echevarría-Zomeño *et al.* 2006) to follow the development of *O. cumana* tubercles for about three weeks, and in pots (10 cm × 10 cm) in an earth-sand-mixture for two months until shoots of *O. cumana* emerged.

Sunflower achenes were moistened for one to two days, peeled and grown on wet filter paper at 25°C. Seedlings with a root length of 2–3 cm were placed in the root chamber between lid and filter paper. The root chambers were made out of sterile Petri dishes (diameter 9 cm) filled with perlite and covered with a wet filter paper (both heat sterilised at 150°C for 2 h) with 1 cm wide holes cut into the upper side of the lid and bottom (Fig. 3.1). The lids were fixated with adhesive tape and the Petri dishes placed vertically in a box. Each chamber was irrigated individually, so that the perlite stayed moist but without excess water collecting in the box.

Seeds of *O. cumana*, pathotype (physiological race) G, collected in 2012 in Russia (kindly provided by Dr. T. Antonova and PhD S. Guchetl), were surface sterilised according to Conn *et al.* 2015 (modified). The seed were treated with 70 % ethanol for 1 min, 3.6 % sodium hypochlorite solution in 0.1 % Tween 80 for 3 min and 30 s in a supersonic bath, followed by 0.01 M hydrochloric acid for 10 min. After each step, seeds were rinsed thoroughly with deionised water.

Inoculation was performed after four to five days, once the sunflower roots reached a length of approximately 6 cm. Surface sterilised *O. cumana* seeds (about 300 seeds per host plant) were placed with a thin spatula on the filter paper of the root chambers within a distance of ca. 2 mm from the roots. For the potted plants, five-day old seedlings were inoculated with a pinch of non-surface sterilised seeds of *O. cumana*, pathotype E+, collected in Spain 2014, in the planting hole.

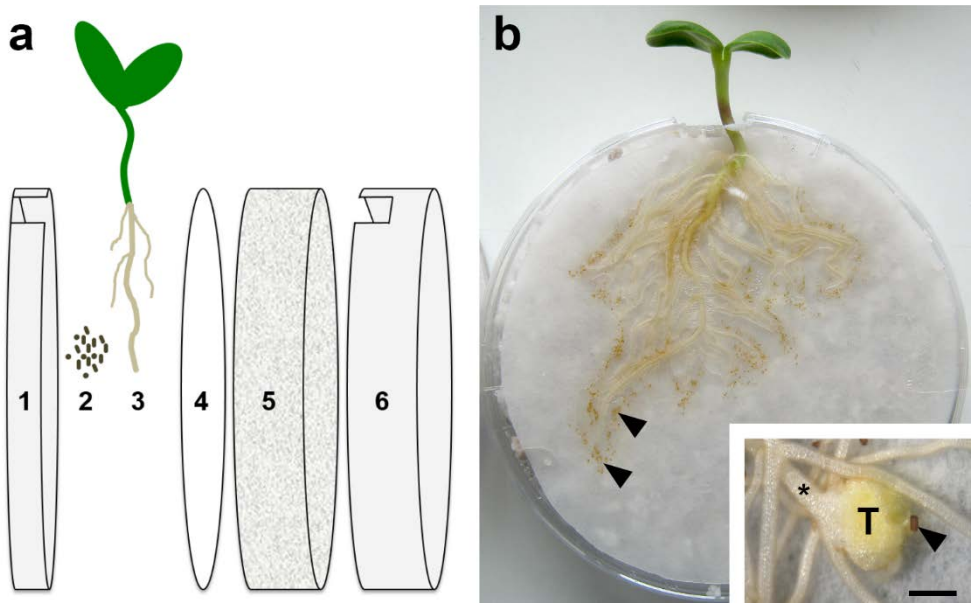

Fig. 3.1 Root chamber cultivation system. **a** Diagram of the root chamber setup: 1 – lid of Petri dish, 2 – surface sterilised seeds of *O. cumana*, 3 – sunflower plant, 4 – filter paper, 5 – perlite, 6 – bottom of Petri dish. **b** Root chamber with a 12 d old sunflower plant and seeds of *O. cumana* (*arrowheads*) placed near the sunflower roots; *inset*: tubercle (*T*) of *O. cumana*, the host root is thickened above the tubercle (*asterisk*); seed coat (*arrowhead*), *scale bar* = 500 µm.

Sample preparation for light- and transmission electron microscopy

Three weeks after inoculation, parasitised sunflower roots were dissected with a razor blade 2 mm above and below the tubercle. For control samples, 12-day old non-infected sunflower roots, 2–3 mm in length, were taken. Sunflower hypocotyl of four-day old seedlings and young *O. cumana* shoots (62 dpi) were cut longitudinally into segments of 1–2 mm length.

For xylem identification, fresh samples of young tubercles were stained by fixing the tissue in ethanol / acetic acid (75 % / 25 %) for 15 min, washing in 0.1 M sodium phosphate buffer (pH 7.2) and incubating in 0.1 % Safranin-O (Chroma, Köngen, Germany) for 5 min at 90°C. After cooling to room temperature, samples were washed in buffer and cleared in chloral hydrate for two days.

For serial sectioning, the samples were fixed in 2.5 % glutaraldehyde in 0.1 M sodium phosphate buffer (pH 7.2) for at least 1 h, washed with buffer and postfixed in 1 % osmium tetroxide in 0.1 M sodium phosphate buffer for 1 h. Subsequently, the samples were washed in distilled water and dehydrated using the progressive lowering temperature technique (1–2 h in 30 % ethanol at 0°C, 1–2 h in 50 % ethanol at -20°C, overnight in 70 % ethanol at -35°C, 1.5 h in 100 % ethanol at -35°C). After adjusting to room temperature, the samples were infiltrated with LR-White resin (Science Service, Munich, Germany) in three steps (50 %, 75 % and 100 % LR-White in ethanol for 3 h, respectively) and polymerised in gelatine capsules at 60°C for 24 h.

Careful trimming and serial sectioning of the samples was necessary to locate the connecting tissues in the tubercles and the phloem in sunflower roots, hypocotyl and *O. cumana* shoots. Longitudinal and cross sections were prepared using an ultratom (Ultracut UCT, Leica, Wetzlar, Germany) with a diamond histo knife (Diatome ultra 35°, Science Service, Munich, Germany). Semithin sections (1 µm) were collected on glass slides, stained for 1 h with 0.05 % Toluidine blue (Merck, Darmstadt, Germany) and investigated with an Axioplan microscope (Zeiss, Göttingen, Germany) coupled to a digital camera (Leica DCM 2900, Wetzlar, Germany).

Semithin sections containing phloem of *O. cumana* shoots were stained for starch using potassium triiodide according to Lugol (Ruzin 1999).

Ultrathin sections of about 80 nm thickness were collected on Pioloform-carbon-coated copper or nickel grids and stained for 10 min with uranyl acetate and for 90 s with lead citrate. They were examined using an EM 10 transmission electron microscope (Zeiss, Oberkochen, Germany). Photos were taken with a digital camera (Megaview II, Soft Imaging System, Münster, Germany) or by 8 × 9 cm TEM negatives, which were digitised with an Epson Perfection 2450 scanner. Photoshop CC 2015.5 (Adobe systems, San José, CA, USA) was used to adjust brightness, contrast and white balance of the micrographs.

Several transmission electron micrographs were merged using the "Photomerge" function of Photoshop to obtain larger overview images.

Sieve-element plastid size measurement and statistics

Size (length and width) of sieve-element plastids of *H. annuus* roots (n=29), *O. cumana* shoots (n=15) and tubercles (n=24) was measured on transmission electron micrographs (Adobe Photoshop CC2015.5) and statistically treated (mean value and standard deviation). Analysis of variance (ANOVA) was conducted on the plastid length and width with InfoStat (Version 2016e, InfoStat Group, University of Córdoba, Argentina). Effects were considered significant if $p < 0.05$ in the Tukey test.

3. 3 Results

A special root chamber cultivation system was used to obtain samples of the host-parasite complex (Fig. 3.1). Due to the intermingled tissue organization between the *O. cumana* haustorium and the *H. annuus* root, the phloem connection was difficult to localise. Therefore, first the phloem anatomy and ultrastructure of sunflower roots and broomrape tubercles were investigated independently to identify differentiating features which could allow assignment in the interaction zone.

The phloem in sunflower roots was aligned with the xylem in the vascular bundle (Fig. 3.2 a), thus corresponding to the anatomy of a typical dicotyledonous root showing star-shaped central xylem with two or four rays and phloem patches in between (Fig. 3.2 b). The cell types of the phloem, i.e. sieve-tube elements, companion cells and phloem-parenchyma cells, could be distinguished ultrastructurally. Sieve-tube elements of sunflower (hereafter abbreviated as sieve elements) contained plastids with characteristic starch inclusions, round mitochondria, a sieve plate with callose-lined sieve pores and filamentous P-protein (Fig. 3.2 c). There was no difference in the ultrastructure of sieve elements of roots and hypocotyl.

In the *O. cumana* haustorium and tubercle, the vascular arrangement was more complex (Fig. 3.3). In whole mount samples, phloem was not detectable, but strands of xylem connected tubercle and haustorium to the host xylem (Fig. 3.3 a). In serial sections of a somewhat larger tubercle, sieve elements were identified ultrastructurally and marked red on the adjacent semithin sections (Fig. 3.3 c–e). Single strands of phloem meandered

spirally through the tubercle without association to the xylem strands. Based on this observation, a sketch of the phloem arrangement in host and parasite was constructed (white lines in Fig. 3.3 b).

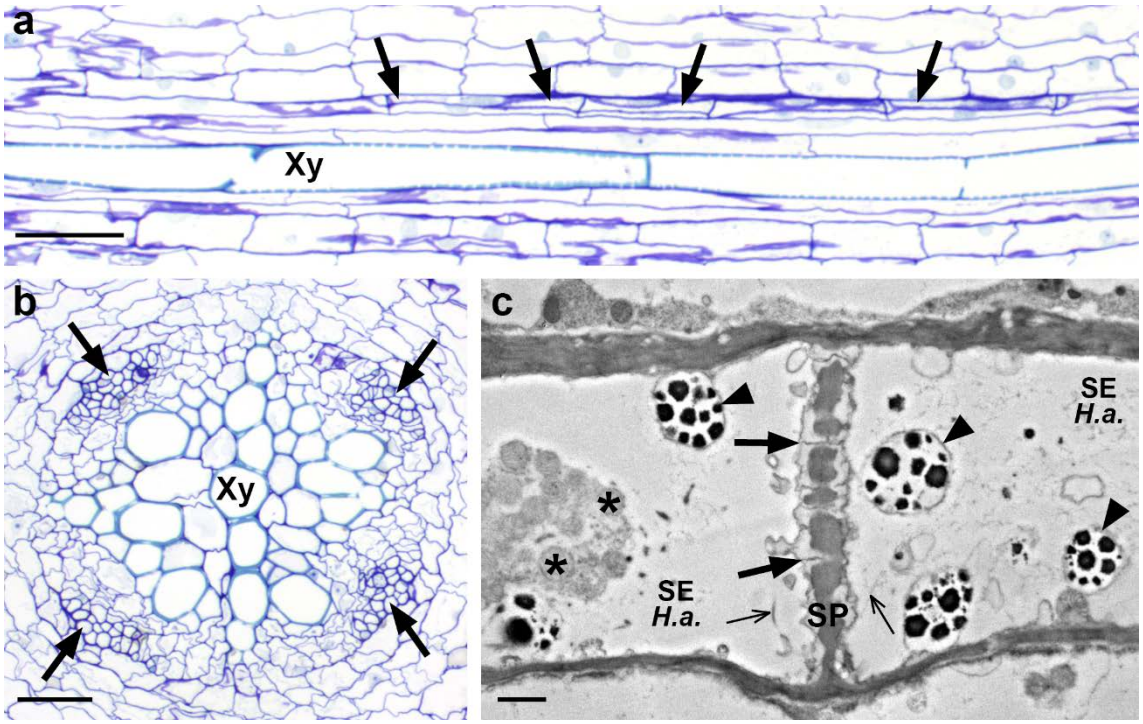

Fig. 3.2 Position and characteristics of phloem in sunflower host roots. **a** Sieve elements (*arrows*) in the vascular bundle; xylem (*Xy*), light micrograph, longitudinal section, *scale bar* = 50 µm. **b** Vascular bundle with four strands of phloem (*arrows*) around the xylem (*Xy*); light micrograph, cross section, *scale bar* = 50 µm. **c** Sieve elements of *H. annuus* (*SE H.a.*) with typical sieve-element plastids (*arrowheads*), round mitochondria (*asterisks*), filamentous P-protein (*thin arrows*) and sieve plate (*SP*) with callose-lined sieve pores (*bold arrows*); transmission electron micrograph of a longitudinal section, *scale bar* = 1 µm.

The ultrastructure of sieve-tube elements in *O. cumana* tubercles and shoots revealed all typical features of angiosperm sieve elements (Fig. 3.4): lack of nuclei and vacuoles, sieve plates with sieve pores that were evenly lined with callose (Fig. 3.4 b, d, h and i, *arrows*), round mitochondria (Fig. 3.4 a, *asterisks*), filamentous P-protein (Fig. 3.4 h, *thin arrows*) and typical sieve-element plastids (Fig. 3.4 a, b, c, e, f, g, i and j). Sieve-element plastids of *O. cumana* contained starch inclusions which could be verified by the classical iodine staining. Starch grains in sieve-element plastids appeared reddish black, whereas in the proplastids of parenchymatic cells they stained bluish black (Fig. 3.4 j). The density of the sieve-element plastid matrix varied between the developmental stages: in tubercles, the matrix usually was transparent (Fig. 3.4 a–c), whereas in the shoot it ranged from

transparent to grainy (Fig. 3.4 e–g). The number of starch inclusions in one section ranged from one to about six. The inclusions had a symmetric granulous appearance with uneven edges (e.g. Fig 4 b and g) and differed from the amorphous ultrastructure of amyloplast starch (Fig. 3.4 a, *black arrowheads*) or the homogenous inclusions found in proplastids (Fig. 3.4 e and j, *black arrowheads*), which were the other plastid types found in *O. cumana* tissues.

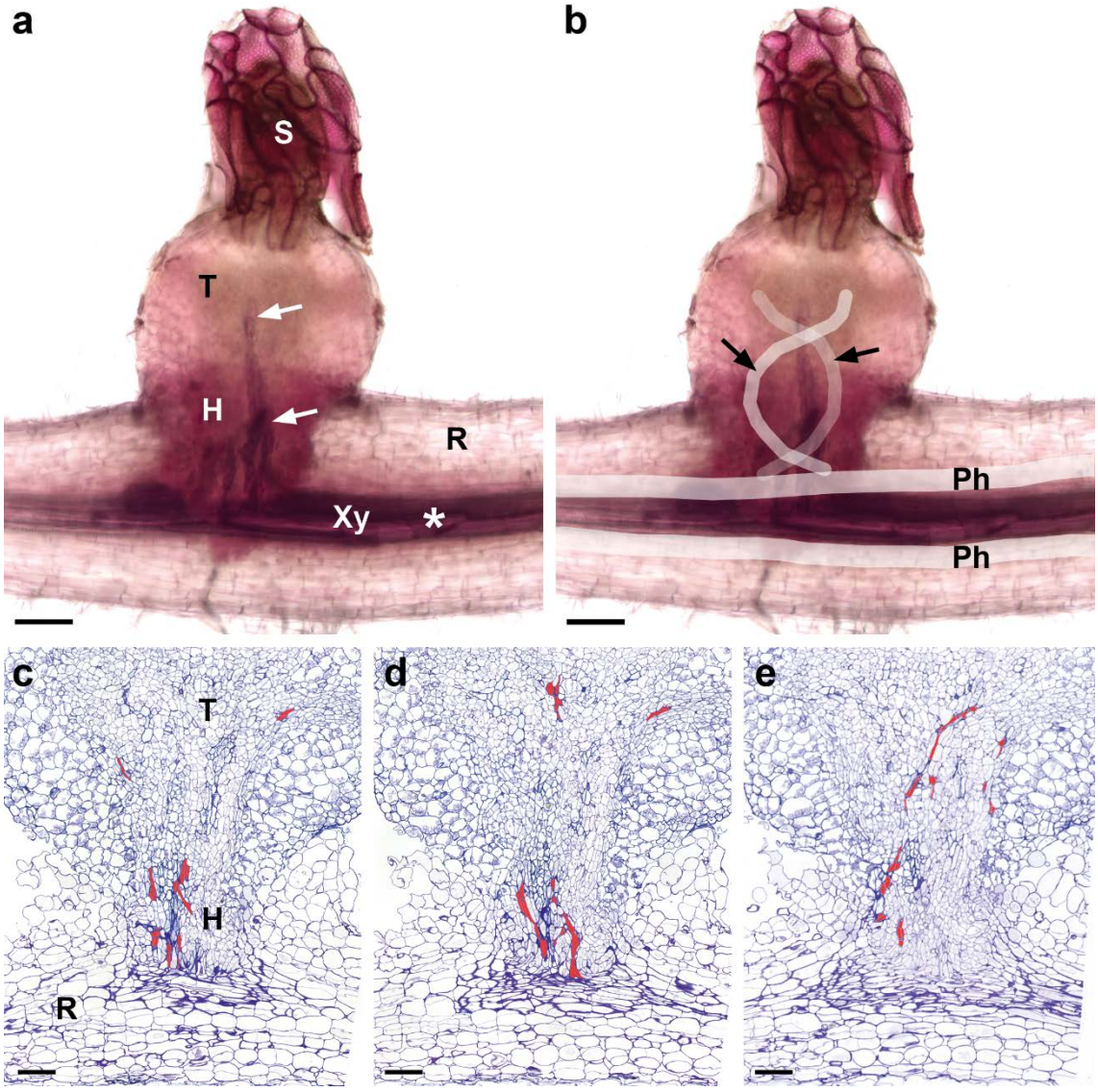

Fig. 3.3 Arrangement of phloem and xylem in haustoria and tubercles of *O. cumana*. **a** Whole mount of an *O. cumana* tubercle (*T*) on an *H. annuus* root (*R*). Xylem (*Xy*) is stained dark red. Single xylem strands (*white arrows*) connect root and tubercle via the haustorium (*H*). Host xylem is more abundant upstream of the haustorium (*asterisk*). **b** Sketch (*white lines*) of phloem (*Ph*) in the host root and single phloem strands in the tubercle (*black arrows*). **c–e** Serial sections of a tubercle (*T*) and haustorium (*H*) on the host root (*R*). Sieve elements, identified ultrastructurally on adjacent ultrathin sections, are marked red. Light micrographs of longitudinal sections, *scale bars* = 100 µm.

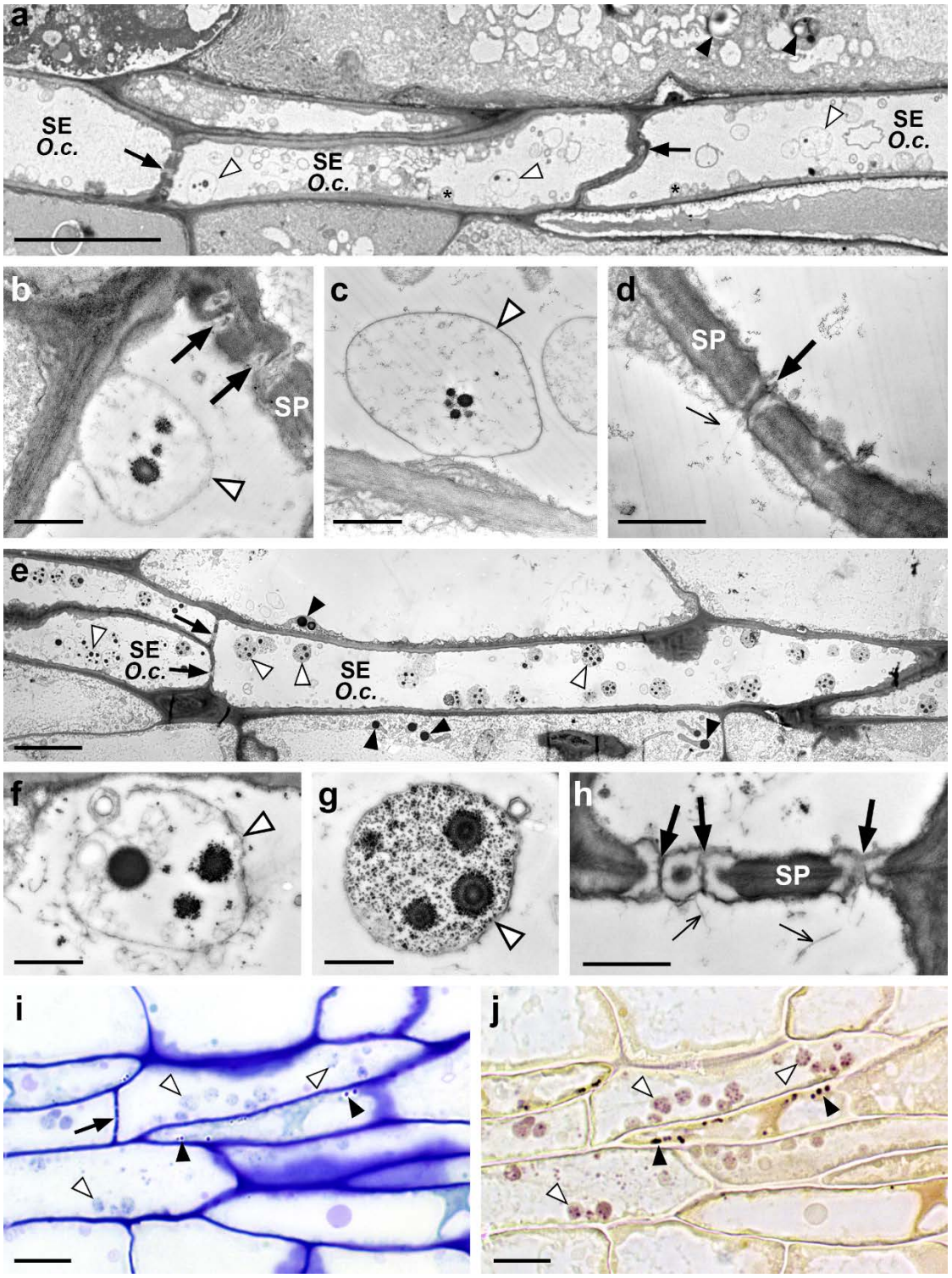

Fig. 3.4 Sieve elements of *O. cumana* tubercles and shoots. **a–h** Transmission electron micrographs. **a** Sieve elements (*SE O.c.*) in the tubercle with typical sieve-element plastids (*white arrowheads*); sieve plates (*arrows*), amyloplasts (*black arrowheads*) in parenchyma cell, *scale bar* = 10 µm. **b–d** Tubercle sieve-element plastids (*white arrowheads*) and sieve plates (*SP*) with sieve pores (*bold arrows*); P-protein (*thin arrow*), *scale bars* = 1 µm. **e** Sieve elements (*SE O.c.*) in the shoot with sieve-element plastids (*white arrowheads*) and sieve plates (*arrows*); proplastids (*black arrowheads*) in parenchyma cells, *scale bar* = 10 µm. **f–g** Shoot sieve-element plastids (*white arrowheads*); *scale bars* = 1 µm. **h** Sieve plate (*SP*) with typical callose (white) around the sieve pores (*bold arrows*); P-protein (*thin arrows*), *scale bar* = 1 µm. **i–j** Light micrographs of phloem in the shoot; sieve-element plastids (*white arrowheads*), proplastids (*black arrowheads*) in parenchyma cell, sieve plate (*arrow*), *scale bars* = 10 µm. **i** Toluidine blue staining. **j** Lugol's iodine staining.

Sieve-element plastids of *O. cumana* and *H. annuus* were significantly different in size, plastids of *O. cumana* being larger than those of *H. annuus* (Fig. 3.5 a). They also showed differences in ultrastructure. The typical plastids of *H. annuus* had a round shape and contained numerous large starch inclusions (Fig. 3.5 b), whereas those of *O. cumana* often had a more irregular shape and contained fewer starch inclusions that were often smaller (Fig. 3.5 c).

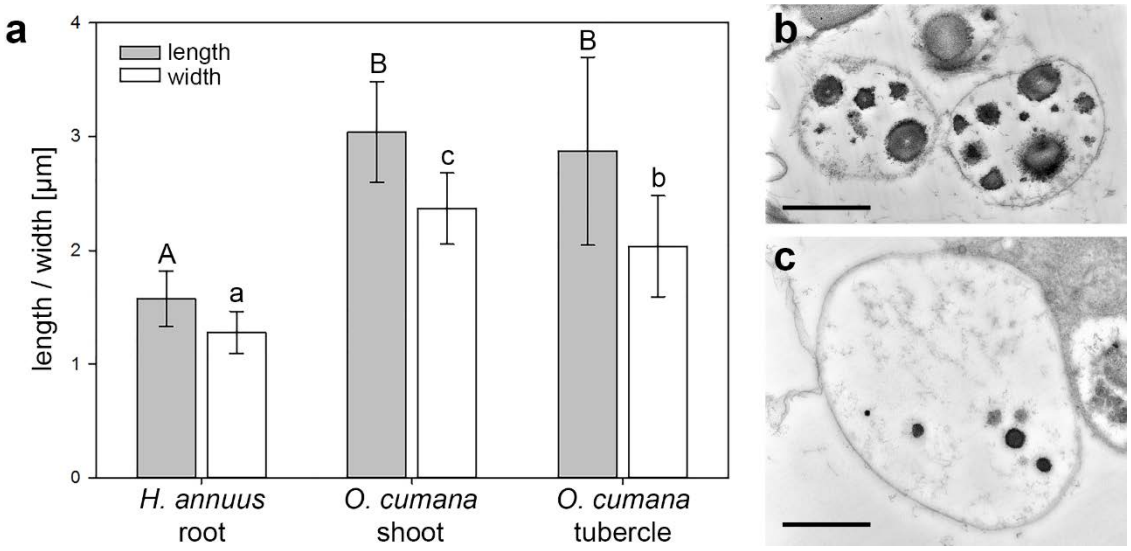

Fig. 3.5 Size and ultrastructure of sieve-element plastids of *H. annuus* and *O. cumana*. **a** Sieve-element plastid length (*grey*) and width (*white*); means ± standard deviation. The same letter (capitals for length and lowercase for width) indicates that differences are not statistically significant (Tukey test, $p < 0.05$). **b** Transmission electron micrograph of an *H. annuus* sieve-element plastid. **c** Transmission electron micrograph of an *O. cumana* sieve-element plastid; *scale bars* = 1 µm.

Direct sieve element connections between host and parasite could be identified by their typical sieve-element plastids (Fig. 3.6, Table 3.1), although at connection sites between haustorium and root, parasite and host tissues were intermingled and their origin was very difficult to distinguish by their position or shape. Therefore, a series of micrographs with increasing magnification was used to follow the route of the phloem (shown in Fig. 6–8). Haustorial sieve elements of *O. cumana* were narrow and elongated (Fig. 3.6 c). Due to their winding arrangement in the tubercle, the sieve tubes were often not sectioned longitudinally and appeared isodiametrical or irregular in shape in the outer parts of the haustorium (Fig. 3.6 c, upper sieve elements). Haustorial sieve elements showed the same

ultrastructure as in the tubercle and had irregularly-shaped plastids with a transparent matrix and few starch inclusions (Fig. 3.6 d–e).

Sieve elements of *H. annuus* and *O. cumana* were connected by interspecific sieve plates (Fig. 3.7). The sieve plates showed more callose around the sieve pores on the host side (Fig. 3.7 c and e). This phenomenon could also be observed at sieve plates between fully differentiated host and developing parasite sieve elements (Fig. 3.7 d and f). In contrast, pores in sieve plates of *H. annuus* sieve elements (Fig. 3.2 c) and that of *O. cumana* (Fig. 3.4 d and h) were evenly lined with callose.

The development of the phloem connection between host and parasite could be observed in serial sections (Fig. 3.8). Parenchymatic haustorial cells still containing a nucleus, vacuoles and dense cytoplasm were connected to fully differentiated host sieve elements (Fig. 3.8 c–d) via callose-lined pores that resembled those in interspecific sieve plates between fully differentiated sieve elements (Fig. 3.8 f–g).

Host and parasite showed cell proliferation. At the contact site, the host root was thickened above the tubercle (Fig. 3.1 b, *inset*) and showed more xylem vessels (Fig. 3.3 a–b). Near the haustorium, the number of sieve elements of the host root was increased (Fig. 3.8 f).

Table 3.1 Traits used to distinguish *H. annuus* from *O. cumana* sieve elements (*SE*). Sieve-element plastid size is given in µm, means ± standard deviation, n=29 for *H. annuus*, n=41 for *O. cumana*

trait	***H. annuus***	***O. cumana***	**shown in**
size of SE plastids	1.57±0.24 × 1.28±0.19	2.94±0.70 × 2.16±0.43	Fig. 3.5 a
shape of SE plastids	round	often more irregular	Fig. 3.2 c, Fig. 3.4 b, c, f, g, Fig. 3.5 b, c, Fig. 3.6 d, e
number of SE plastid starch inclusions	numerous	few	Fig. 3.2 c, Fig. 3.4 b, c, f, g, Fig. 3.5 b, c, Fig. 3.6 d, e
size of SE plastid starch inclusions	large	usually smaller	Fig. 3.2 c, Fig. 3.4 b, c, f, g, Fig. 3.5 b, c, Fig. 3.6 d, e
callose deposition at interspecific sieve plate	more	less	Fig. 3.7 e, f, Fig. 3.8 d, g

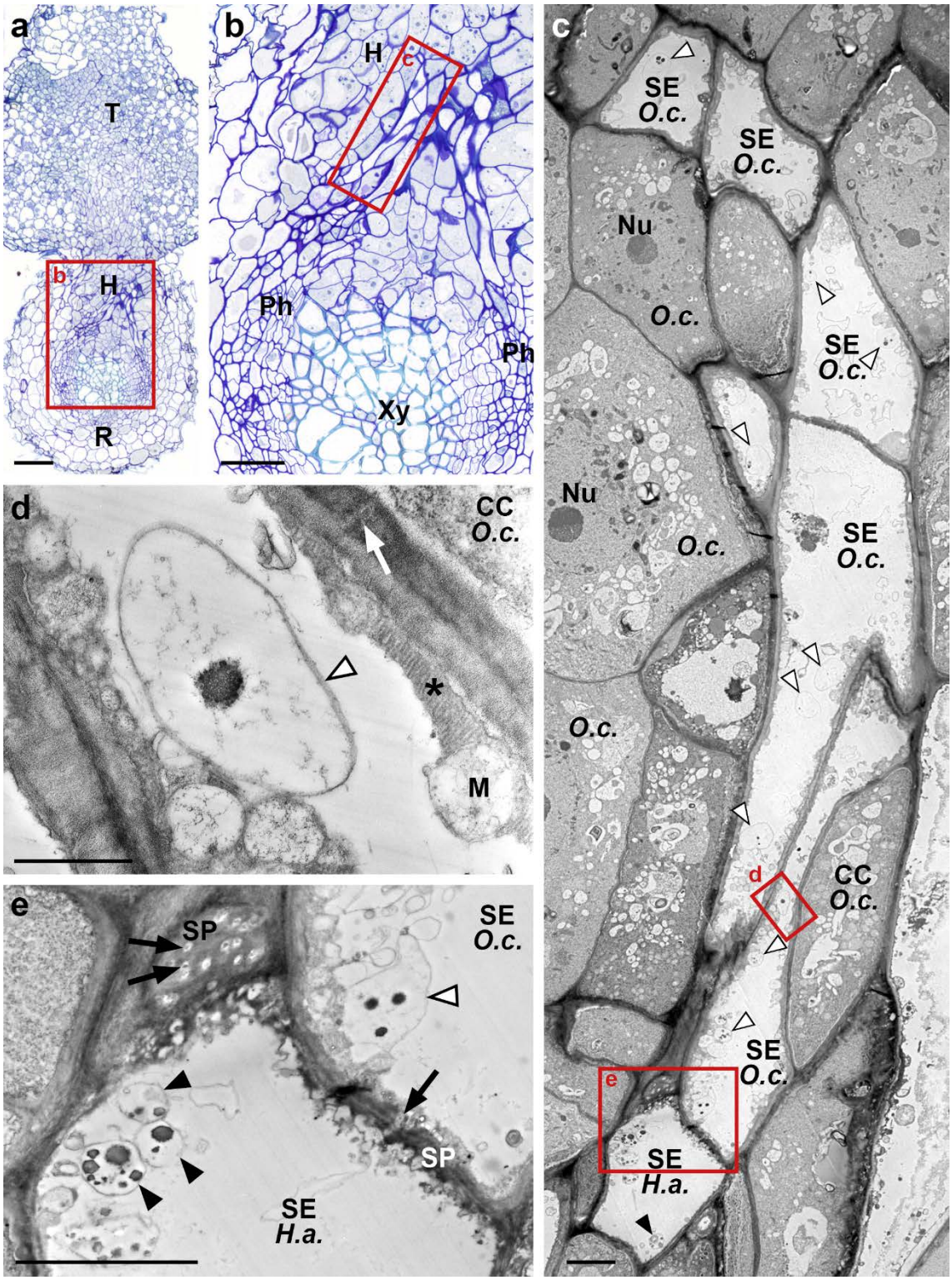

Fig. 3.6 Direct sieve-element connection between the host and the parasite. **a** Light micrograph of an *O. cumana* tubercle (*T*) and haustorium (*H*, longitudinal section) in a host root (*R*, cross section); *scale bar* = 100 µm. **b** Detail of *a*, showing the haustorium (*H*) and the vascular bundle of the host root; xylem (*Xy*), phloem (*Ph*), *scale bar* = 50 µm. **c** Transmission electron micrograph of the haustorial sieve-element connection (serial section 1 (*CC O.c.*); plasmodesmata (*white arrow*), sieve-element plastid (*white arrowhead*), roundish mitochondria (*M*), sieve-element reticulum (*asterisk*), *scale bar* = 1 µm. **e** Detail of *c*. Sieve elements of *H. annuus* (*SE H.a.*) and *O. cumana* (*SE O.c.*) with their typical plastids (*arrowheads*) are connected via sieve pores (*black arrow*). In the upper half, the sieve plate (*SP*) is cut tangentially and shows typical callose (white) around the sieve pores (*black arrows*); *scale bar* = 5 µm.

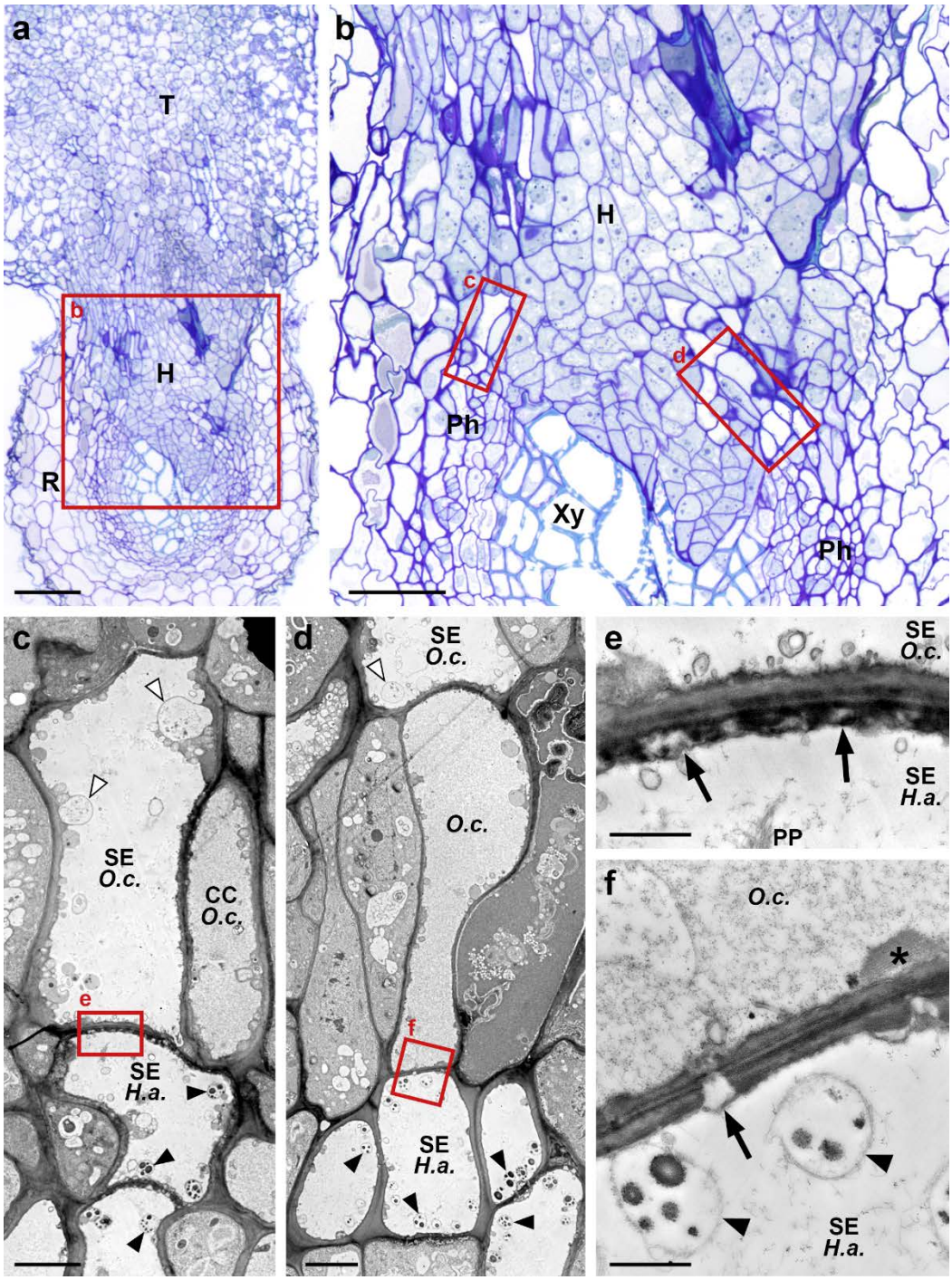

Fig. 3.7 Interspecific sieve-plate ultrastructure. **a** Light micrograph of an *O. cumana* tubercle (*T*) and haustorium (*H*, longitudinal section) in an *H. annuus* host root (*R*, cross section); *scale bar* = 100 µm. **b** Detail of *a*, showing the haustorium (*H*) and the vascular bundle of the host root; xylem (*Xy*), phloem (*Ph*); *scale bar* = 50 µm. **c** Transmission electron micrograph (serial section near *b*) of the haustorial sieve element (*SE O.c.*) in direct contact with a host sieve element (*SE H.a.*, transversally cut); typical host sieve-element plastids (*black arrowheads*), typical sieve-element plastids of *O. cumana* (*white arrowheads*), companion cell (*CC O.c.*), *scale bar* = 5 µm. **d** Transmission electron micrograph (serial section near *b*) of a developing haustorial sieve element (*O.c.*) in contact with a fully developed sieve element of the host (*SE H.a.*) and a sieve element of *O. cumana* (*SE O.c.*); sieve-element plastids of *O. cumana* (*white arrowheads*), sieve-element plastids of *H. annuus* (*black arrowheads*), *scale bar* = 5 µm. **e** Detail of *c*. The interspecific sieve plate showing more callose (*arrows*) on the host side; P-protein (*PP*), *scale bar* = 1 µm. **f** Detail of *d*. A developing haustorial sieve element (*O.c.*) in contact with a fully developed sieve element of the host (*SE H.a.*). Sieve plate with more callose (*arrow*) on the host side; sieve-element reticulum (*asterisk*), sieve-element plastids (*black arrowheads*), *scale bar* = 1 µm.

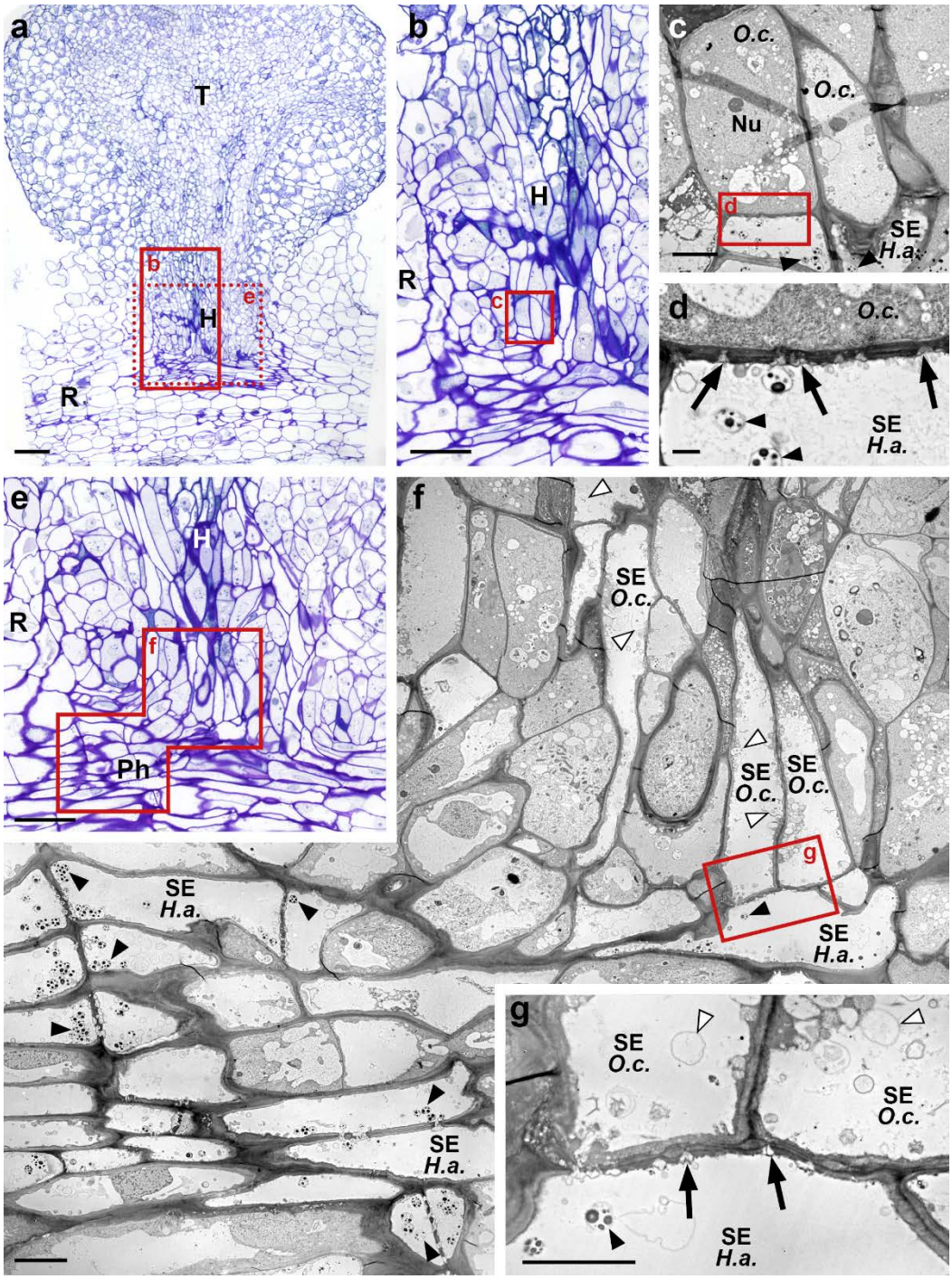

Fig. 3.8 Development of the sieve element connection between host and parasite. **a** Light micrograph of an *O. cumana* tubercle (*T*) and haustorium (*H*) in an *H. annuus* host root (*R*); longitudinal section, *scale bar* = 100 µm. **b** Detail of *a*. Haustorium (*H*) in the host root (*R*); *scale bar* = 50 µm. **c** Transmission electron micrograph of a serial section near *b* showing the connection between a parenchymatic *O. cumana* cell (*O.c.*) to a fully differentiated *H. annuus* sieve element (*SE H.a.*); nucleus (*Nu*), sieve-element plastids of *H. annuus* (*black arrowheads*), *scale bar* = 10 µm. **d** Detail of *c*. Interspecific sieve plate development between a parenchymatic *O. cumana* cell and an *H. annuus* sieve element (*SE H.a.*) with more callose on the host side (*arrows*); sieve-element plastids (*black arrowheads*), *scale bar* = 1 µm. **e** Light micrograph, detail of a serial section near *a*. Haustorium (*H*) in contact with the host root (*R*) phloem (*Ph*); *scale bar* = 50 µm. **f** Transmission electron micrograph of a serial section near *e*. Direct connection between *O. cumana* sieve elements (*SE O.c.*) and *H. annuus* sieve elements (*SE H.a.*); sieve-element plastids (*arrowheads*), *scale bar* = 10 µm. **g** Detail of *f*. Fully developed interspecific sieve plates; *O. cumana* sieve elments (*SE O.c.*), *H. annuus* sieve element (*SE H.a.*); sieve pores with more callose on the host side (*arrows*), sieve-element plastids (*arrowheads*), *scale bar* = 5 µm.

3. 4 Discussion

A functioning phloem connection is of utmost importance for the survival of an annual holoparasite such as *O. cumana*, which has to complete its lifecycle in a short period of time strictly by means of nutrients acquired from its host. Such a massive translocation of nutrients requires an effective transport route, i.e. an efficient connection to the host's phloem. Contrary to xylem, which is easily visible under the light microscope due to its characteristic wall thickenings that can be stained with various techniques (for example Musselman & Dickison 1975, Zhou *et al.* 2004, Bar-Nun *et al.* 2008, Spallek *et al.* 2017), phloem is much more difficult to detect. This is especially true for the haustorium-host root-complex, because both host and parasite show cell proliferation, tissues are intermingled and phloem is arranged spirally without association with the xylem. The sieve-element plastid was used as an ultrastructural cell marker to trace the exact connection point between foreign sieve elements.

Sieve-element plastid ultrastructure has been used as a taxonomic tool since the 1970s (Behnke 1981). The inclusions in these plastids can be protein, protein and starch, or just starch, resulting in a classification system of P-type (with several subtypes and forms) or S-type plastids, where no forms have been defined (Behnke 1981). Sieve-element plastid starch differs from amyloplast starch in its chemistry and ultrastructure. In contrast to the amorphous appearance of amyloplast starch, sieve-element starch forms more regular, granulous starch grains that consist of highly branched molecules with numerous α-(1→6)-linkages (Palevitz & Newcomb 1970). In the study of *O. crenata* tubercles on *V. narbonensis*, distinction of host and parasite sieve elements was possible due to the different plastid types, with P-type plastids in the host and S-type plastids in the parasite. Furthermore, P-protein ultrastructure differed greatly, with filamentous P-protein in *O. crenata* and typically cristalline P-protein bodies in *V. narbonensis* (Dörr & Kollmann 1995). In contrast, sunflower has S-type plastids and filamentous P-protein (Kollmann & Glockmann 1990), which made a distinction of host and parasite sieve elements in the interaction with *O. cumana* more difficult. Close examination of sieve-element plastid ultrastructure in the different organs of sunflower and *O. cumana*, however, showed a clear difference in plastid size, shape and the number of their starch inclusions. While sieve-element plastids of *H. annuus* did not vary between organs, the plastids of *O. cumana* differed between tubercle and shoot, with a transparent matrix in tubercles and haustoria and a matrix with variable density, but mostly granular, in shoots. This

could be related to the developmental processes of plastid differentiation (Kollmann *et al.* 1983). Varying matrix density was also observed in developing *Phaseolus vulgaris* L. sieve-element plastids (Palevitz & Nowcomb 1970) and in sieve-element plastids of wound phloem in *Pisum sativum* L. (Schulz 1986).

Interestingly, the function of sieve-element plastids is not known. One opinion is that they do not have any function (Behnke 1990, Sjölund 1997), but it is also hypothesised that they could play a role in sieve plate occlusion during injury or as storage organelles (Knoblauch & van Bel 1998, van Bel 2003, Knoblauch & Peters 2010).

Another helpful tool to locate phloem connections in the haustorium was the specific ultrastructure of the sieve plate. While callose lining of the sieve pores was relatively even in intraspecific sieve plates, it was more irregular in the interspecific sieve plates with more callose on the host side. This phenomenon was also described for the interaction of *O. crenata* with *V. narbonensis* (Dörr & Kollmann 1995). Interspecific sieve pores form from secondary plasmodesmata, a process that has been described for graft unions (Kollmann & Glockmann 1990) and seems to follow the same differentiation principle that has been described for primary sieve pores (Esau & Thorsch 1985).

For parasitic plants, the question arose whether young parenchymatic parasite cells could connect to fully differentiated host sieve elements, or if synchronous development of sieve elements is necessary to establish the connection. For *O. crenata*, Dörr & Kollmann (1995) found interspecific plasmodesmata between parenchymatic host and parasite cells, but no connection between parenchymatic parasite cells and mature host sieve elements. In this study, cytoplasmic connections between parenchymatic haustorial cells as well as young parasite sieve elements to fully differentiated host sieve elements were found, thus confirming that *O. cumana* cells can connect to mature host phloem tissue.

The sieve plate formed between *O. cumana* and sunflower sieve elements ensures a direct, symplastic contact between host and parasite and allows the parasite to obtain nutrients. Tracer experiments with *P. aegyptiaca* and *P. ramosa* showed transfer of proteins and fluorescent symplastic tracer from the host phloem to *Phelipanche* tubercles, thus demonstrating the symplastic phloem continuity (Aly *et al.* 2011, Péron *et al.* 2017). It would be interesting to combine physiological and ultrastructural experiments on the phloem connection of parasitic plants to show what implication haustorium anatomy has for nutrient and macromolecule transfer.

For a long time, it was believed that differentiated phloem does not occur at the haustorial interface (Kuijt 1991). This has been ruled out by the current study which supports the findings on *O. crenata* (Dörr & Kollmann 1995) and hints at a wider occurrence of direct phloem connections in the terminal haustoria of *Orobanche* species.

II. Conclusions

In this thesis, three main questions about the biology of the early *O. cumana*-sunflower-interaction could be answered.

After the first important step in the parasite's lifecycle, host-induced germination, the second step is finding the host root by chemotropism. *O. cumana* germtubes showed a positive chemotropic response to sunflower sesquiterpene lactones. This confers a double role to sesquiterpene lactones as chemical signals for *O. cumana* germination and chemotropism and sheds light on an important step in the interaction of root parasitic plants with their hosts, which has not received research attention in the last decades.

Germination and chemotropism, however, were not the decisive steps in the incompatible interaction of the resistant sunflower line examined in this thesis. Instead, the sunflower resistance mechanism manifested itself in the host root cortex, where the development of the haustorium stopped before reaching the vascular bundle. How this new resistance mechanism works was not detectable by means of fluorescence- or transmission electron microscopy. Unravelling this mechanism in future experiments will require immuno-histological techniques or expression studies with tissue of the host-pathogen-interface and can provide relevant information for sunflower breeding.

The key organ for parasitic plants is the haustorium which enables transfer of water, minerals and organic nutrients from the host to the parasite. Whereas xylem connections are relatively easy to study, phloem connections are difficult to detect. To tell if a sieve element belongs to the host or the parasite requires ultrastructural markers, such as sieve-element plastids that differ between taxa. In this thesis, a method was established to identify sieve elements of sunflower and *O. cumana* based on their ultrastructure. Hence it was possible to locate the exact connecting site between host and parasite phloem and to identify a direct symplastic connection between the two plant species. This new knowledge on the ultrastructure of the phloem connection is the basis for further physiological experiments that can deepen our understanding of parasitic plants.

All in all, the answers to the research questions that were found in this thesis can provide relevant information for plant breeding, plant physiology and botany in general.

III. References

Aber M, **Sallé** G (**1982**) Etude histo-cytologique des principaux stades phénologiques d'*Orobanche crenata* Forsk.. Biol Cell 44:21a

Aly R, Goldwasser Y, Eizenberg H, Hershenhorn J, Golan S, Kleifeld Y (**2001**) Broomrape (*Orobanche cumana*) control in sunflower (*Helianthus annuus*) with imazapic. Weed Technol 15:306–309

Aly R, Hamamouch N, Abu-Nassar J, Wolf S, Joel DM, Eizenberg H, Kaisler E, Cramer C, Gal-On A, Westwood, JH (**2011**) Movement of protein and macromolecules between host plants and the parasitic weed *Phelipanche aegyptiaca* Pers.. Plant Cell Rep 30:2233–2241

Amri M, Abbes Z, Youssef SB, Bouhadida M, Salah HB, Kharrat M (**2012**) Detection of the parasitic plant, *Orobanche cumana* on sunflower (*Helianthus annuus* L.) in Tunisia. Afr J Biotechnol 11(18):4163–4167

Antonova TS (**2014**) The history of interconnected evolution of *Orobanche cumana* Wallr. and sunflower in the Russian Federation and Kazakhstan. Helia 37(61):215–225

Antonova TS, **ter Borg** SJ (**1996**) The role of peroxidase in the resistance of sunflower against *Orobanche cumana* in Russia. Weed Res 36:113–121

Attawi FAJ (**1977**) Morphologisch-anatomische Untersuchungen über den Parasitismus, die Entwicklungsweise und die Struktur der Haustorialorgane von *Orobanche*-Arten sowie über Samenstrukturen bei Orobanchaceae. Dissertation, Gießen, Germany

Auger B, Pouvreau JB, Pouponneau K, Yoneyama K, Montiel G, Le Bizec B, Yoneyama K, Delavault P, Delourme R, Simier P (**2012**) Germination stimulants of *Phelipanche ramosa* in the rhizosphere of *Brassica napus* are derived from the glucosinolate pathway. Mol Plant Microbe Interact 25(7):993–1004

Ba AT (**1988**) Structure et ultrastructure de l'haustorium de *Striga hermonthica*, une scrophulariacée parasite du mil (*Pennisetum typhoides*). Can J Bot 66:2111–2117

Bar-Nun N, Sachs T, Mayer AM (**2008**) A Role for IAA in the infection of *Arabidopsis thaliana* by *Orobanche aegyptiaca*. Ann Bot 101:261–265

Beck-Mannagetta G (**1890**) Monographie der Gattung *Orobanche*. Bibliotheca Botanica, Vol. 19, Theodor Fischer, Cassel

Behnke H-D (**1981**) Sieve-element characters. Nord J Bot 1(3):381–400

Behnke H-D (**1990**) Siebelemente – Kernlose Spezialisten für den Stofftransport in Pflanzen. Naturwiss 77:1–11

van Bel AJE (**2003**) The phloem, a miracle of ingenuity. Plant Cell Environ 26:125–149

Bertsch B (**2015**) Wirtsfindung durch Chemotropismus bei der Sonnenblumen-Sommerwurz *Orobanche cumana* Wallr. Thesis for a teaching degree, Institute of Botany, University of Hohenheim, Germany

ter Borg SJ (**1986**) Present and future of *Orobanche* research; summary and conclusions. In: ter Borg SJ (ed) Proceedings of a workshop on biology and control of *Orobanche*. LH/VPO, Wageningen, The Netherlands, pp 196–203

Botha PJ (**1948**) The parasitism of *Alectra vogelii* Benth., with special reference to the germination of its seeds. Jour S Afr Bot 14:63–80

Cantamutto M, Miladinovic D, Antonova T, Pacureanu M, Molinero Ruiz L, Kaya Y, Seiler GJ (**2014**) Agroecology of broomrape *Orobanche cumana* distribution in five continents. In: Proceedings of the third international symposium on broomrape (*Orobanche* spp.) in sunflower. Córdoba, Spain, pp 104–109

Conn CE, Bythell-Douglas R, Neumann D, Yoshida S, Whittington B, Westwood JH, Shirasu K, Bond CS, Dyer KA, Nelson DC (**2015**) Convergent evolution of strigolactone perception enabled host detection in parasitic plants. Science 349(6247):540–543

Cook CE, Whichard LP, Turner B, Wall ME, Egley GH (**1966**) Germination of witchweed (*Striga lutea* Lour.): isolation and properties of a potent stimulant. Science 154:1189–1190

Cook CE, Whichard LP, Wall ME, Egley GH, Coggon P, Luhan PA, McPhail, AT (**1972**) Germination stimulants. II. The structure of strigol – a potent seed germination stimulant for witchweed (*Striga lutea* Lour.). J Am Chem Soc 94:6198–6199

Delavault P (**2015**) Knowing the parasite: biology and genetics of *Orobanche*. Helia 38(62):15–29

Dörr I (**1990**) Sieve elements in haustoria of parasitic angiosperms. In: Behnke HD, Sjolund RD (eds) Sieve elements – comparative structure, induction and development. Springer, Berlin, pp 239–256

Dörr I, Visser JH, Kollmann R (**1979**) On the parasitism of *Alectra vogelii* Benth. (Scrophulariaceae) – III. The occurrence of phloem between host and parasite. Z Pflanzenphysiol 94:427–439

Dörr I, Staack A, Kollmann R (**1994**) Resistance of *Helianthus* to *Orobanche* – histological and cytological studies. In: Pieterse, AH, Verkleij JAC, ter Borg SJ (eds) Biology and management of *Orobanche*, Proceedings of the third international workshop on *Orobanche* and related *Striga* research. Royal Tropical Institute, Amsterdam, The Netherlands, pp 276–289

Dörr I, **Kollmann** R (**1975**) Strukturelle Grundlagen des Parasitismus bei *Orobanche* – II. Die Differenzierung der Assimilat-Leitungsbahn im Haustorialgewebe. Protoplasma 83(3):185–199

Dörr I, **Kollmann**, R (**1995**) Symplasmic sieve element continuity between *Orobanche* and its host. Bot Acta 108:47–55

Duca M, Port A, Boicu A, Sestacova T (**2017**) Molecular characterization of broomrape populations from Republic of Moldova using SSR markers. Helia 40(66):47–59

Echevarría-Zomeño S, Pérez-de-Luque A, Jorrín J, Maldonado AM (**2006**): Pre-haustorial resistance to broomrape (*Orobanche cumana*) in sunflower (*Helianthus annuus*): cytochemical studies. J Exp Bot 57(15):4189–4200

Eizenberg H, Hershenhorn J, Plakhine D, Kleinfeld Y, Shtienberg D, Rubin B (**2003a**) Effect of temperature on susceptibility of sunflower varieties to sunflower broomrape (*Orobanche cumana*) and Egyptian broomrape (*Orobanche aegyptiaca*). Weed Science 51:279–286

Eizenberg H, Plakhine D, Hershenhorn J, Kleinfeld Y, Rubin B (**2003b**) Resistance to broomrape (*Orobanche* spp.) in sunflower (*Helianthus annuus* L.) is temperature dependent. J Exp Bot 54(385):1305–1311

Ekawa M, **Aoki** K (**2017**) Phloem-conducting cells in haustoria of the root-parasitic plant *Phelipanche aegyptiaca* retain nuclei and are not mature sieve elements. Plants 6(60): 1–12

Esau K, **Thorsch** J (**1985**) Sieve plate pores and plasmodesmata, the communication channels of the symplast: ultrastructural aspects and developmental relations. Amer J Bot 72(10):1641–1653

Fernández-Aparicio M, Flores F, Rubiales D (**2009**) Recognition of root exudates by seeds of broomrape (*Orobanche* and *Phelipanche*) species. Ann Bot 103:423–431

Fernández-Martínez JM, Velasco L, Pérez-Vich B (**2012**) Progress in research on breeding for resistance to sunflower broomrape. Helia 35(57):47–56

Fernández-Martínez JM, Pérez-Vich B, Velasco L (**2015**) Sunflower broomrape (*Orobanche cumana* Wallr.). In: Martínez-Force E, Dunford NT, Salas JJ (eds) Sunflower oilseed. Chemistry, production, processing and utilization. AOCS Press, Champaign, IL, USA, pp 129–156

Gagne G, Roeckel-Drevet P, Grezes-Besset B, Shindrova P, Ivanov P, Grand-Ravel C, Vear F, Tourvieille de Labrouhe D, Charmet G, Nicolas P (**1998**) Study of the variability and evolution of *Orobanche cumana* populations infesting sunflower in different European countries. Theor Appl Genet 96(8):1216–1222

Goldwasser Y, **Rodenburg** J (**2013**) Integrated agronomic management of parasitic weed seed banks. In: Joel DM, Gressel J, Musselman LJ (eds) Parasitic Orobanchaceae – parasitic mechanisms and control strategies. Springer, Berlin, pp 393–413

Gurrata P (**2016**) Vergleich der Interaktion zweier Rassen von *Orobanche cumana* Wallr. mit Sonnenblumen unterschiedlicher Resistenz. Master thesis, Institute of Botany, University of Hohenheim, Germany

Heide-Jørgensen HS (**2008**) Parasitic flowering plants. Brill, Leiden

Heide-Jørgensen HS (**2013**) Introduction: the parasitic syndrome in higher plants. In: Joel DM, Gressel J, Musselman LJ (eds) Parasitic Orobanchaceae – parasitic mechanisms and control strategies. Springer, Berlin, pp 1–18

Höniges A, Wegmann K, Ardelean A (**2008**) *Orobanche* resistance in sunflower. Helia 31(49):1–12

Imerovski I, Dimitrijevic A, Miladinovic D, Dedic B, Jocic S, Kovacevic B, Obreht D (**2013**) Identification of PCR markers linked to different *Or* genes in sunflower. Plant Breed 132:115–120

Jan CC, **Seiler** GJ (**2007**) Sunflower. In: Singh, RJ (ed) Genetics resources, chromosome engineering, and crop improvement. Vol. 4: Oilseed crops. CRC Press, Taylor and Francis Group, New York, pp 103–165

Jebri M, Ben Khalifa M, Fakhfakh H, Pérez-Vich B, Velasco L (**2017**) Genetic diversity and race composition of sunflower broomrape populations from Tunisia. Phytopathol Mediterr 56(3):421–430

Jestin C, Lecompte V, Duroueix F (**2014**) Current situation of sunflower broomrape in France. In: Proceedings of the third international symposium on broomrape (*Orobanche* spp.) in sunflower. Córdoba, Spain, pp 28–31

Joel DM (**2013**) Functional structure of the mature haustorium. In: Joel DM, Gressel J, Musselman LJ (eds) Parasitic Orobanchaceae – parasitic mechanisms and control strategies. Springer, Berlin, pp 25–60

Joel DM, Hershenhorn J, Eizenberg H, Aly R, Ejeta G, Rich PJ, Ransom JK, Sauerborn J, Rubiales D (**2007**) Biology and management of weedy root parasites. In: Janick J (ed) Horticultural Reviews, Vol. 33, pp 267–349

Joel DM, Chaudhuri SK, Plakhine D, Ziadna H, Steffens JC (**2011**) Dehydrocostus lactone is exuded from sunflower roots and stimulates germination of the root parasite *Orobanche cumana*. Phytochemistry 72:624–634

Joel DM, **Bar** H (**2013**) The seed and the seedling. In: Joel DM, Gressel J, Musselman LJ (eds) Parasitic Orobanchaceae – parasitic mechanisms and control strategies. Springer, Berlin, pp 147–165

Joel DM, **Losner-Goshen** D (**1994**) The attachment organ of the parasitic angiosperms *Orobanche cumana* and *O. aegyptiaca* and its development. Can J Bot 72:564–574

Kadry, AER, **Tewfic** H (**1956**) A contribution to the morphology and anatomy of seed germination in *Orobanche crenata*. Bot Notiser 109(4):385–399

Katzir N, Portnoy V, Tzuri G, Joel DM, Castejón-Muñoz M (**1996**) Use of random amplified polymorphic DNA (RAPD) markers in the study of the parasitic weed *Orobanche*. Theor Appl Genet 93(3):367–372

Kaya Y (**2014**) Current situation of sunflower broomrape around the world. In: Proceedings of the third international symposium on broomrape (*Orobanche* spp.) in sunflower. Córdoba, Spain, pp 9–18

Knoblauch M, **van Bel** AJE (**1998**) Sieve tubes in action. Plant Cell 10:35–50

Knoblauch M, **Peters** WS (**2010**) Münch, morphology, microfluids – our structural problem with the phloem. Plant Cell Environ 33:1439–1452

Koch L (**1887**) Die Entwicklungsgeschichte der Orobanchen, mit besonderer Berücksichtigung ihrer Beziehungen zu den Kulturpflanzen. Carl Winter's Universitätsbuchhandlung, Heidelberg

Kollmann R, Dörr I, Schulz A, Behnke HD (**1983**) Funktionelle Differenzierung der Assimilatleitbahnen. Ber Deutsch Bot Ges 96:117–132

Kollmann R, **Glockmann** C (**1990**) Sieve elements of graft unions. In: Behnke HD, Sjolund RD (eds) Sieve elements – comparative structure, induction and development. Springer, Berlin, pp 219–237

Kreutz CAJ (**1995**) *Orobanche cumana* In: *Orobanche* – The European broomrape species – A field guide. Vol. 1: Central and Northern Europe. Stichting Natuurpublicaties Limburg, Maastricht, The Netherlands, pp 88–89

Krupp A (**2014**) Interaktion der Sonnenblumen-Sommerwurz (*Orobanche cumana* Wallr.) mit verschiedenen Wirts-Genotypen. Master thesis, Institute of Botany, University of Hohenheim, Germany

Krupp A, Rücker E, Heller A, Spring O (**2014**) Seed structure characteristics of *Orobanche cumana* populations. Helia 38(62):1–14

Krupp A, Heller A, Spring O (**2019**) Development of phloem connection between the parasitic plant *Orobanche cumana* and its host sunflower. Protoplasma 256:1385–1397

Kuijt J (**1969**) The biology of parasitic flowering plants. University of California Press, Berkely

Kuijt J (**1991**) The haustorial interface: what does it tell us? In: Ransom JK, Musselman LJ, Worsham AD, Parker C (eds) Proceedings of the 5th international symposium of parasitic weeds. Nairobi, Kenya, CIMMYT, pp 1–5

Labrousse P, Arnaud MC, Serieys H, Bervillé H, Thalouarn P (**2001**) Several mechanisms are involved in resistance of *Helianthus* to *Orobanche cumana* Wallr.. Annals of Botany 88:859–868

Labrousse P, Delmail D, Arnaud MC, Thalouarn P (**2010**) Mineral nutrient concentration influences sunflower infection by broomrape (*Orobanche cumana*). Botany 88:839–849

Letousey P, de Zélicourt A, Vieira Dos Santos C, Thoiron S, Monteau F, Simier P, Thalouarn P, Delavault P (**2007**) Molecular analysis of resistance mechanisms to *Orobanche cumana* in sunflower. Plant Pathol 56:536–546

Losner-Goshen D, Joel DM, Mayer AM, Steffens JC (**1991**) Surface characteristics and internal structure of *Orobanche* seedlings. Proceedings of the 5th international symposium of parasitic weeds. Nairobi, Kenya, CIMMYT, pp 356–360

Losner-Goshen D, Portnoy VH, Mayer AM, Joel DM (**1998**) Pectolytic activity by the haustorium of the parasitic plant *Orobanche* L. (Orobanchaceae) in host roots. Ann Bot 81:319–326

Meier CS (**2018**) Nachweis von Sesquiterpenlactonen in Samen, Keimlingen und Ölen von *Helianthus annuus*. Bachelor thesis, Institute of Botany, University of Hohenheim, Germany

Molinero-Ruiz L, García-Carneros AB, Collado-Romero M, Raranciuc S, Dominguez J, Melero-Vara JM (**2013**) Pathogenic and molecular diversity in highly virulent populations of the parasitic weed *Orobanche cumana* (sunflower broomrape) from Europe. Weed Res 54:87–96

Molinero-Ruiz L, Delavault P, Pérez-Vich B, Păcureanu-Joiţa M, Bulos M, Altieri E, Domínguez J (**2015**) History of the race structure of *Orobanche cumana* and the breeding of sunflower for resistance to this parasitic weed: a review. Span J Agric Res 13(4):e10R01

Musselman LJ, **Dickison** WC (**1975**) The structure and development of the haustorium in parasitic Scrophulariaceae. Bot J Linn Soc 70:183–212

Nabloussi A, Velasco L, Assissel N (**2018**) First report of sunflower broomrape, *Orobanche cumana* Wallr., in Morocco. Plant Dis 102(2):457–457

Păcureanu-Joiţa M, Raranciuc S, Sava E, Stanciu D, Nastase D (**2009**) Virulence and aggressiveness of sunflower broomrape (*Orobanche cumana* Wallr.) populations in Romania. Helia 32(51):111–118

Padilla-Gonzalez GF, dos Santos FA, Da Costa FB (**2016**) Sesquiterpene lactones: more than protective plant compounds with high toxicity. Crit Rev Plant Sci 35(1):18–37

Palevitz BA, **Newcomb** EH (**1970**) A study of sieve element starch using sequential enzymatic digestion and electron microscopy. J Cell Biol 45:383–398

Parker C (**2009**) Observations on the current status of *Orobanche* and *Striga* problems worldwide. Pest Manag Sci 65:453–459

Parker C (**2013**) The parasitic weeds of the Orobanchaceae. In: Joel DM, Gressel J, Musselman LJ (eds) Parasitic Orobanchaceae – parasitic mechanisms and control strategies. Springer, Berlin, pp 313–344

Parker C, **Riches** CR (**1993**) Parasitic weeds of the world: biology and control. CAB Int, Wallingford, UK

Pearson HHW (**1913a**) The problem of the witchweed. Agr J Union South Africa 6(5):803–805

Pearson HHW (**1913b**): On the problem of witchweed. Science Bulletin 40:1–34

Pérez-de-Luque A, Jorrín J, Cubero JI, Rubiales D (**2005**) *Orobanche crenata* resistance and avoidance in pea (*Pisum* spp.) operate at different developmental stages of the parasite. Weed Res 45:379–387

Pérez-de-Luque A, Lozano MD, Moreno MT, Tastillano PS, Rubiales D (**2007**) Resistance to broomrape (*Orobanche crenata*) in faba bean (*Vicia faba*): cell wall changes associated with prehaustorial defensive mechanisms. Ann Appl Biol 151:89–98

Pérez-de-Luque A, Fondevilla S, Pérez-Vich B, Aly R, Thoiron S, Simier P, Castillejo MA, Fernández-Martínez JM, Jorrín J, Rubiales D, Delavault P (**2009**) Understanding *Orobanche* and *Phelipanche*-host plant interactions and developing resistance. Weed Res 49(Suppl. 1):8–22

Pérez-Vich B, Akhtouch B, Knapp, SJ, Leon AJ, Velasco L, Fernández-Martínez JM, Berry ST (**2004**) Quantitative trait loci for broomrape (*Orobanche cumana* Wallr.) resistance in sunflower. Theor Appl Genet 109:92–102

Pérez-Vich B, Velasco L, Rich PJ, Ejeta G (**2013**) Marker-assisted and physiology-based breeding for resistance to root parasitic Orobanchaceae. In: Joel DM, Gressel J, Musselman LJ (eds) Parasitic Orobanchaceae – parasitic mechanisms and control strategies. Springer, Berlin, pp 369–391

Péron T, Candat A, Montiel G, Veronesi C, Macherel D, Delavault P, Simier P (**2017**) New insights into phloem unloading and expression of sucrose transporters in vegetative sinks of the parasitic plant *Phelipanche ramosa* L. (Pomel). Front Plant Sci 7:2048, 15 pp.

Pineda-Martos R, Velasco L, Fernández-Escobar J, Fernández-Martínez JM, Pérez-Vich B (**2013**) Genetic diversity of *Orobanche cumana* populations from Spain assessed using SSR markers. Weed Res 53:279–289

Porterfield DM, **Musgrave** ME (**1998**) The tropic response of plant roots to oxygen: oxytropism in *Pisum sativum* L. Planta 206:1–6

Pujadas-Salvà AJ, **Velasco** L (**2000**) Comparative studies on *Orobanche cernua* L. and *O. cumana* Wallr. (Orobanchaeceae) in the Iberian Peninsula. Bot J Linn Soc 134:513–527

Raupp FM, **Spring** O (**2013**) New sesquiterpene lactones from sunflower root exudate as germination stimulants for *Orobanche cumana*. J Agr Food Chem 61:10481–10487

Rodríguez-Ojeda MI, Fernández-Martínez JM, Velasco L, Pérez-Vich B (**2013**) Extent of cross-fertilization in *Orobanche cumana* Wallr.. Biol Plant 57(3):559–562

Román B, Alfaro C, Torres AM, Moreno MT, Satovic Z, Pujadas A, Rubiales D (**2003**) Genetic relationships among *Orobanche* species as revealed by RAPD analysis. Ann Bot 91:637–642

Runyon, JB, Mescher MC, De Moraes CM (**2006**) Volatile cues guide host location and host seletion by parasitic plants. Science 313:1964–1967

Ruyter-Spira C, Kohlen W, Charnikhova T, van Zeijl A, van Bezouwen L, de Ruijter N, Cardoso C, Lopez-Raez JA, Matusova R, Bours R, Verstappen F, Bouwmeester H (**2011**) Physiological effects of the synthetic strigolactone analog GR24 on root system architecture in *Arabidopsis*: another belowground role for strigolactones? Plant Physiol 155:721–734

Ruzin SE (**1999**) Plant microtechnique and microscopy. Oxford University Press, New York, pp 154–155

Sauerborn J, Buschmann H, Ghiasvand Ghiasi K, Kogel KH (**2002**) Benzothiadiazole activates resistance in sunflower (*Helianthus annuus*) to the root-parasitic weed *Orobanche cumana*. Phytopathol 92:59–64

Saunders AR (**1933**) Studies in phanerogamic parasitism, with particular reference to *Striga lutea* Lour. South African Department of Agriculture Science Bulletin 128, 56 pp.

Schädlich M (**2013**) Erfassung von Keimstimulantien für *Orobanche cumana* in Exsudaten von Sonnenblumen. Master thesis, Institute of Botany, University of Hohenheim, Germany

Schmauder K (**2015**) Genexpressions- und Metabolitmuster von Sesquiterpenlactonen in Keimlingen der Sonnenblume. Master thesis, Institute of Botany, University of Hohenheim, Germany

Schulz A (**1986**) Wound phloem in transition to bundle phloem in primary roots of *Pisum sativum* L. – I. Development of bundle-leaving wound-sieve tubes. Protoplasma 130:12–26

Serghini K, Pérez-de-Luque A, Castejón-Muñoz M, García-Torres L, Jorrín JV (**2001**) Sunflower (*Helianthus annuus* L.) response to broomrape (*Orobanche cernua* Loefl.) parasitism: induced synthesis and excretion of 7-hydroxylated simple coumarins. J Exp Bot 52(364):2227–2234

Shi BX, Chen GH, Zhang ZJ, Hao JJ, Jing L, Zhou HY, Zhao J (**2015**) First report of race composition and distribution of sunflower broomrape, *Orobanche cumana*, in China. Plant Dis 99(2):291–291

Siame BP, Weerasuriya Y, Wood K, Ejeta G, Butler LG (**1993**) Isolation of strigol, a germination stimulant for *Striga asiatica*, from host plants. J Agric Food Chem 41:1486–1491

Sisou D, Tadmor Y, Eizenberg H (**2019**) Characterization of resistance to sunflower broomrape (*Orobanche cumana* W.) in sunflower (*Helianthus annuus* L.). In: 15th World congress on parasitic plants, Amsterdam, The Netherlands, p 12

Sjölund RD (**1997**) The phloem sieve element: a river runs through it. Plant Cell 9:1137–1146

Škorić D, Păcureanu-Joiţa M, Salva E (**2010**) Sunflower breeding for resistance to broomrape (*Orobanche cumana* Wallr.). Analele I.N.C.D.A. Funduela 78(1):63–79

Smith LV (**2018**) Sesquiterpenlactone in Samen und Öl von *Helianthus annuus* L. und ihre Beteiligung in Wachstumsprozessen. Thesis for a teaching degree, Institute of Botany, University of Hohenheim, Germany

Spallek T, Melnyk CW, Wakatake T, Zhang J, Sakamoto Y, Kiba T, Yoshida S, Matsunaga S, Sakakibara H, Shirasu K (**2017**) Interspecies hormonal control of host root morphology by parasitic plants. PNAS 114(20):5283–5288

Spring O, Gómez-Zeledón J, Hadžiabdić D, Trigiano RN, Thines M, Lebeda A (**2018**) Biological characteristics and assessment of virulence diversity in pathosystems of economically important biotrophic oomycetes. Crit Rev Plant Sci 37(6):439–495

Spring O, **Hager** A (**1981**) Inhibition of elongation growth by two sesquiterpene lactones isolated from *Helianthus annuus* L. Planta 156:433–440

Teryokhin ES (**1997**) Weed broomrapes – systematics, ontogenesis, biology, evolution. Aufstiegs-Verlag, Germany

Thorogood CJ, Rumsey FJ, Hiscock SJ (**2009**) Seed viability determination in parasitic broomrapes (*Orobanche* and *Phelipanche*) using fluorescein diacetate staining. Weed Res 49:461–468

Timko MP, **Scholes** JD (**2013**) Host reaction to attack by root parasitic plants. In: Joel DM, Gressel J, Musselman LJ (eds) Parasitic Orobanchaceae – parasitic mechanisms and control strategies. Springer, Berlin, pp 115–141

Ueno K, Furumoto T, Umeda S, Mizutani M, Takikawa H, Batchvarova R, Sugimoto Y (**2014**) Heliolactone, a non-sesquiterpene lactone germination stimulant for root parasitic weeds from sunflower. Phytochem 108:122–128

Velasco L, Pérez-Vich B, Jan CC, Fernández-Martínez JM (**2007**) Inheritance of resistance to broomrape (*Orobanche cumana* Wallr.) race F in a sunflower line derived from wild sunflower species. Plant Breed 126:67–71

Véronési C, Bonnin E, Benharrat H, Fer A, Thalouarn P (**2005**) Are pectolytic enzymes of *Orobanche cumana* seedlings related to virulence towards sunflower? Israel J Plant Sci 53:19–27

Visser JH, Dörr I, Kollmann R (**1977**) On the parasitism of *Alectra vogelii* Benth. (Scrophulariaceae). Early development of the primary haustorium and initiation of the stem. Zeitschr Pflanzenphysiol 84:213–222

Wegmann K (**1986**). Biochemistry of osmoregulation in *Orobanche* and possible biochemical basis of *Orobanche* resistance. In: S.J. ter Borg (eds) Proceedings of a Workshop on Biology and Control of *Orobanche*, Wageningen, The Netherlands, pp 107–113

Westwood JH (**2013**) The physiology of the estalished parsite-host-association. In: Joel DM, Gressel J, Musselman LJ (eds) Parasitic Orobanchaceae – parasitic mechanisms and control strategies. Springer, Berlin, pp 87–114

Whitney PJ, **Carsten** C (**1981**) Chemotropic response of broomrape radicles to host root exudates. Ann Bot 48:919–921

Williams CN (**1961**) Tropism and morphogenesis of *Striga* seedlings in the host rhizosphere. Ann Bot 25:407–415

Yoneyama K, Ruyer-Spira C, Bouwmeester H (**2013**) Induction of germination. In: Joel DM, Gressel J, Musselman LJ (eds) Parasitic Orobanchaceae – parasitic mechanisms and control strategies. Springer, Berlin, pp 167–194

Yoshida S, Cui S, Ichihashi Y, Shirasu K (**2016**) The haustorium, a specialized invasive organ in parasitic plants. Annu Rev Plant Biol 67:643–667

Yoshida S, **Shirasu** K (**2009**) Multiple layers of incompatibility to the parasitic witchweed, *Striga hermonthica*. New Phytologist 183:180–189

de Zélicourt A, Letousey P, Thoiron S, Campion C, Simoneau P, Elmorjani K, Marion D, Simier P, Delavault P (**2007**) Ha-DEF1, a sunflower defensin, induces cell death in *Orobanche* parasitic plants. Planta 226:591–600

Zhou WJ, Yoneyama K, Takeuchi Y, Iso S, Rungmekarat S, Chae SH, Sato D, Joel DM (**2004**) In vitro infection of host roots by differentiated calli of the parasitic plant *Orobanche*. J Exp Bot 55(398):899–907

IV. Acknowledgements

I am deeply grateful to my supervisor **Prof. Dr. Otmar Spring** for letting me work on *Orobanche cumana* and for his constant support, even after his retirement.

Many thanks to **Prof. Dr. Philipp Schlüter**, who supported me in the final phase of my PhD. It is a pleasure working with you.

I also want to express my gratitude to **Prof. Dr. Joachim Sauerborn**, who offered guidance during the beginning of my PhD, and to **PD Dr. Frank Rasche** for taking the role of additional examiner.

I am deeply grateful to **Dr. Anne Heller** for everything she taught me and for the wonderful working atmosphere in the electron microscopy lab.

The financial support of the "Water – People – Agriculture" Research Training Group funded by the **Anton & Petra Ehrmann-Stiftung** is gratefully acknowledged, as well as the friendliness of everyone in **WPA**: Prof. Dr. Folkard Asch, Dr. Marcus Giese, Alexandra Schappert, Saskia Windisch and of course my fellow scholars: Carolin Weiler, Charles Nwankwo, Hongxi Liu, Irene Witte, Katja Beck, Kevin Thellmann Konrad Egenolf, Laura Mack, Robert Kahle, Sarah Glatzle *et al.*

Thank you to **Patrizia Dach** (née Gurrata) and **Barbara Bertsch** for their diligent work in the lab on *O. cumana* during their theses.

I thank **Thomas Spallek** for fruitful discussions about parasitic plants.

A big 'thank you!' goes to all the wonderful members of the **Institute of Botany** – may it rest in peace – who have become like a second family, who shared my joy over good results and lessened my frustration when experiments did not work out:
Daniel Reichle, **Susanne Liner** and **Gabi Eisele** – you were the heart and soul of the institute.

In the working groups of Prof. Spring, Dr. Heller and Prof. Schlüter my thanks go to **Reinhard Zipper**, **Erika Rücker** and **Bärbel Rassow** for technical support, to **my dear colleagues** Adriana Boicu (née Acciu), Evelyn Amrehn, Fabian Runge, Javier Gómez, Katharina Aschenbrenner, Marion Heller-Dohmen, Maximilian Frey and Wolfgang Grasse and of course all the nice students who made life in the lab more fun: Alevtina, Andrej, Aylin B., Barbara, Carolin, Chengwei, Christoph, David, Katharina S., Laura, Lysanne, Marek, Marlisa, Matthias, Mattia, Navid, Nele, Patrizia, Sandra, Sara, Simon *et al.*

Also to my nice colleagues from the **archaeobotany**, **dendrochronology** and **ecophysiology** working groups – thank you for the good times: Alexander Land, Hans-Peter Stika, Reiner Zimmermann, Sabine Remmele and of course also Aleta, Anne T., Ayça, Aylin G., Dieter, Juliane, Magge, Marian, Mona S., Rhina, Stefan *et al.*

Special thanks to **Armin Niessner** and **Magnus Wachendorf** – life in the office would have been so much less fun without you!

I wish to thank **Silke Horakh** for her generosity and friendliness, and all our nice tours in the Hohenheim Gardens.

I am also grateful to all the people who helped me to learn more about plants in all their aspects – **Christine Pommerer**, **Ina Dinter**, **Reinhard Böcker**, **Robert Gliniars** and **Uwe Schwarz**.

Benjamin Krupp, **Johanne Martens** and **Melina Munz** were invaluable in the final stages of my PhD: Thank you for motivating and helping me!

Last but definitely not least: many thanks to my **friends and family**, who helped me to fight all the inner demons that doing a PhD creates. Thank you Anna, Chrissi, Claudi, Dennis, Eva, Flo, Hanne, Melina, Mona, Silke, Uli. My deep gratitude goes to my parents Simone & Winfried, my brother Benjamin, and my husband **Frank Loebard**, who supported me continuously – without you, I could never have done this.

Eidesstattliche Versicherung

Eidesstattliche Versicherung gemäß § 7 Absatz 7 der Promotionsordnung der Universität Hohenheim zum Dr. rer. nat.

1. Bei der eingereichten Dissertation zum Thema

   „Strategies and Mechanisms of Cellular Interaction between the Parasitic Weed *Orobanche cumana* WALLR. and its Host *Helianthus annuus* L.“

   handelt es sich um meine eigenständig erbrachte Leistung.

2. Ich habe nur die angegebenen Quellen und Hilfsmittel benutzt und mich keiner unzulässigen Hilfe Dritter bedient. Insbesondere habe ich wörtlich oder sinngemäß aus anderen Werken übernommene Inhalte als solche kenntlich gemacht.

3. Ich habe nicht die Hilfe einer kommerziellen Promotionsvermittlung oder -beratung in Anspruch genommen.

4. Die Bedeutung der eidesstattlichen Versicherung und der strafrechtlichen Folgen einer unrichtigen oder unvollständigen eidesstattlichen Versicherung sind mir bekannt.

Die Richtigkeit der vorstehenden Erklärung bestätige ich. Ich versichere an Eides Statt, dass ich nach bestem Wissen die reine Wahrheit erklärt und nichts verschwiegen habe.

_____ _____

Ort und Datum Unterschrift